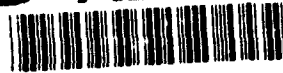


AD-A277 232



2

NAVAL POSTGRADUATE SCHOOL Monterey, California



THESIS

DTIC
SELECTE
MAR 25 1994
S B D

DESIGN OF A TWO DIMENSIONAL PLANER
PRESSURIZED AIR LABYRINTH SEAL TEST RIG

by

Joseph S. Konicki

December 1993

Thesis Advisor:

Knox T. Millsaps, Jr.

Approved for public release; distribution is unlimited.

94 3 24 079

Unclassified

Security Classification of this page

REPORTS DOCUMENTATION PAGE

1a Report Security Classification Unclassified		1b Restrictive Markings	
2a Security Classification Authority		3 Distribution Availability of Report Approved for public release; distribution unlimited.	
2b Declassification/Downgrading Schedule		5 Monitoring Organization Report Number(s)	
6a Name of Performing Organization Naval Postgraduate School	6b Office Symbol (If Applicable) ME	7a Name of Monitoring Organization Naval Postgraduate School	
6c Address (city, state, and ZIP code) Monterey, CA 93943-5000		7b Address (city, state, and ZIP code) Monterey, CA 93943-5000	
8a Name of Funding/ Sponsoring Organization	8b Office Symbol (If Applicable)	9 Procurement Instrument Identification Number	
8c Address (city, state, and ZIP code)		10 Source of Funding Numbers	
Program Element Number	Project No.	Task	Work Unit Accession No.
11 Title (Include Security Classification) Design of a Two Dimensional Planer Pressurized Air Labyrinth Seal Test Rig			
12 Personal Author(s) Joseph S. Konicki			
13a Type of Report Master of Science Thesis	13b Time Covered From To	14 Date of Report (year, month, day) December 1993	15 Page count 87
16 Supplementary Notation The views expressed in this thesis are those of the author and do not reflect the official policy or position of the Department of Defense or the U. S. Government.			
17 Cost Codes:	Field	Group	Subgroup
18 Subject Terms (continue on reverse if necessary and identity by block number) Dump Diffuser, Flow Modification, Laser Doppler Velocimeter, Labyrinth Seal, Leakage Prediction, Pressurized air			
19 Abstract (continue on reverse if necessary and identity by block number) <p>A two-dimensional planer labyrinth seal test rig was designed to operate with air supplied at 45 psig and temperatures up to 150 °F. The rig operates with a manually specified test section pressure up to 30 psig yielding Mach numbers to 0.9 and gap Reynolds numbers to 100,000. The air flow rate through the seal will be controlled by setting inlet pressure and adjusting an outlet control valve. The test section measurements are 18 inches wide by 1.5 inches depth by 6 inches in length and provides for 10:1 large scale geometry seals to be used to facilitate measurements. Design maximum seal gap size is 0.15 inches. The test section has a glass viewing port to allow flow field measurement by non-intrusive means such as Laser Doppler Velocimeter (LDV) with seals containing up to 5 sealing knives. Measurements of pressure, temperature and flow fields can also be simultaneously measured by probes inserted in the seal itself, or mounted on the removable/replaceable top plate. Inlet flow is conditioned through the use of a dump diffuser incorporating screens, honeycombs, expansion and contraction portions. The inlet flow to the test section can be modified from uniform to various non-uniform conditions by employing profile generators such as screens and winglets. A detailed mechanical design has been conducted including stress analysis and seal flow rate predictions.</p>			
20 Distribution/Availability of Abstract X unclassified/unlimited same as report DTIC users		21 Abstract Security Classification Unclassified	
22a Name of Responsible Individual Professor K. Millsaps		22b Telephone (Include Area Code) (408) 656-3382	22c Office Symbol ME-MI

DD FROM 1473, 84 MAR

83 APR edition may be used until exhausted

security classification of this page

All other editions are obsolete

Unclassified

Approved for public release; distribution is unlimited

Design of a Two Dimensional Planer
Pressurized Air Labyrinth Seal Test Rig
by

Joseph S. Konicki
Lieutenant , United States Navy
B.S, United States Naval Academy, 1984

Submitted in partial fulfillment of
requirements for the degree of

MASTER OF SCIENCE IN MECHANICAL ENGINEERING

from the

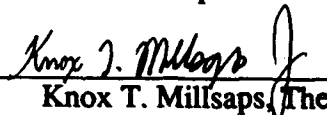
NAVAL POSTGRADUATE SCHOOL

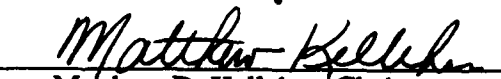
December 1993

Author:


Joseph S. Konicki

Approved by:


Knox T. Millsaps, Thesis Advisor


Matthew D. Kelleher, Chairman,
Department of Mechanical Engineering

ABSTRACT

A two-dimensional planer labyrinth seal test rig was designed to operate with air supplied at 45 psig and temperatures up to 150 °F. The rig operates with a manually specified test section pressure up to 30 psig yielding Mach numbers to 0.9 and gap Reynolds numbers to 100,000. The air flow rate through the seal will be controlled by setting inlet pressure and adjusting an outlet control valve. The test section measurements are 18 inches wide by 1.5 inches depth by 6 inches in length and provides for 10:1 large scale geometry seals to be used to facilitate measurements. Design maximum seal gap size is 0.15 inches. The test section has a glass viewing port to allow flow field measurement by non-intrusive means such as Laser Doppler Velocimeter (LDV) with seals containing up to 5 sealing knives. Measurements of pressure, temperature and flow fields can also be simultaneously measured by probes inserted in the seal itself, or mounted on the removable/replaceable top plate. Inlet flow is conditioned through the use of a dump diffuser incorporating screens, honeycombs, expansion and contraction portions. The inlet flow to the test section can be modified from uniform to various non-uniform conditions by employing profile generators such as screens and winglets. A detailed mechanical design has been conducted including stress analysis and seal flow rate predictions.

Accession For	
NTIS GRA&I	<input checked="checked" type="checkbox"/>
DTIC TAB	<input type="checkbox"/>
Unannounced	<input type="checkbox"/>
Justification	
By	
Distribution	
Availability Codes	
Dist	Avail and/or Special
A-1	

TABLE OF CONTENTS

I.	INTRODUCTION.....	1
II.	BACKGROUND.....	4
III.	DESIGN CALCULATIONS.....	7
	A. CHAPTER OVERVIEW.....	7
	B. DESIGN GOALS.....	7
	C. DESIRED INLET CONDITIONS.....	9
	D. METHODOLOGY.....	9
	E. POSSIBLE APPROACHES.....	10
	F. AIR SUPPLY, PIPING AND VALVES.....	11
	G. DIFFUSER ASSEMBLY.....	14
	H. CONTRACTION SECTION.....	18
	I. SETTLING/MODIFICATION SECTION.....	19
	J. TEST SECTION.....	20
	K. EXIT SECTION.....	21
IV.	DATA ACQUISITION SYSTEM.....	22
	A. ACQUISITION SYSTEM OVERVIEW.....	22
	B. AIRFLOW MEASUREMENT.....	22
	C. FIXED SENSORS.....	23
	D. NON-INTRUSIVE LDV MEASUREMENT	24
V.	PREDICTED TEST RIG PERFORMANCE.....	26
	A. EQUATION DEVELOPMENT	26
	B. PERFORMANCE PREDICTIONS.....	31
VI.	CONCLUSIONS AND RECOMMENDATIONS.....	33
	A. CONCLUSIONS.....	33
	B. RECOMMENDATIONS.....	34

FIGURES.....	35
APPENDIX A: SEAL LEAKAGE PREDICTION PROGRAM.....	70
APPENDIX B: LIST OF MATERIALS.....	72
APPENDIX C: FLOW MODIFICATIONS.....	75
LIST OF REFERENCES.....	76
INITIAL DISTRIBUTION LIST.....	78

LIST OF FIGURES

Figure 1.1	Labyrinth Seal Diagram.....	35
Figure 3.1	Air Supply Facility Diagram.....	36
Figure 3.2	Test Rig Schematic.....	37
Figure 3.3	Manifold Connection Flange.....	38
Figure 3.4	Diffuser Assembly Inlet Plate.....	39
Figure 3.5	Diffuser Assembly Bottom Plate.....	40
Figure 3.6	Diffuser Assembly Top Plate.....	41
Figure 3.7	Diffuser Assembly End Flange.....	42
Figure 3.8	Diffuser Assembly Right Side Plate.....	43
Figure 3.9	Diffuser Assembly Perforation Plates.....	44
Figure 3.10	Diffuser Assembly Perforation Plates.....	45
Figure 3.11	Contraction Section Inlet and Exit Flange.....	46
Figure 3.12	Contraction Cone Side Plate.....	47
Figure 3.13	Settling Section.....	48
Figure 3.14	Test Section Side Plates.....	49
Figure 3.15	Test Section Bottom Plate.....	50
Figure 3.16	Test Section Top Plate.....	51
Figure 3.17	Exit Section Side Plates.....	52
Figure 3.18	Exit Section Top & Bottom Plates.....	53
Figure 3.19	Test Rig Assembly.....	54
Figure 4.1	Data Acquisition Schematic.....	55
Figure 5.1	Labyrinth Seal Diagram.....	56
Figure 5.2	Flow Rate Correlation.....	57
Figure 5.3	Chamber Pressure Correlation.....	58
Figure 5.4	Test Rig Performance ($P_{exit}=5$ psia).....	59

Figure 5.5	Test Rig Performance (Pexit=15 psia).....	60
Figure 5.6	Test Rig Performance (Pexit=25 psia).....	61
Figure 5.7	Test Rig Performance (Pexit=35 psia).....	62
Figure 5.8	Test Rig Performance (Pexit=15 psia, Upper and Lower Bounds).....	63
Figure 5.9	Test Rig Performance (Pexit=15 psia, Low Speed).....	64
Figure 5.10	Test Rig Performance (Back-pressure effects).....	65
Figure 5.11	Test Rig Performance (2 knife seal).....	66
Figure 5.12	Test Rig Performance (3 knife seal).....	67
Figure 5.13	Test Rig Performance (4 knife seal).....	68
Figure 5.14	Test Rig Performance (5 knife seal).....	69

I. INTRODUCTION

There has been rapid development of increasingly more efficient and power dense turbomachinery, particularly in the area of gas turbines. The U.S. Navy is particularly interested in improving turbomachinery since most of its active surface combatants use gas turbines for main propulsion and electrical power generation. In addition, every aircraft in the Navy inventory is driven by some form of gas turbine. Higher efficiency power plants directly translate to better range and longer on-station time without refueling, and lower life cycle operating costs. Higher power density generally results in smaller machinery and increased performance (speed and acceleration) .

Most of the recent advancements in gas turbine efficiency have been realized through increased thermodynamic efficiencies of the components, higher cycle pressure ratios, and higher turbine inlet temperatures. Significant resources are continuing to be directed toward improved turbomachinery. For example, a jet engine manufacturer may spend tens of millions of dollars and years of research in an attempt to improve the efficiency of a gas turbine compressor by only a fraction of a percent. In most cases the risk level is very high since there is no guarantee that further development will improve the efficiency. While most of the losses in efficiency are due to the losses generated in the primary air flow path, some interstage losses occur as a result of ineffective sealing between higher and lower pressure sides across each stage. Non-contact labyrinth seals are typically employed, and are one method to minimize the interstage losses (and improve efficiency) within a gas turbine by reducing this high to low pressure leakage. Figure 1.1 is a two dimensional representation of a 3 dimensional annular labyrinth seal. The object of this seal is to minimize flow rate by successively throttling the flow in one or more chambers to destroy kinetic energy. Most approaches to increasing seal effectiveness pertain to closing the sealing gap, adding more "torturous" passages, and increasing the

size of the chambers. Reduction of interstage losses lead directly to improved compressor and turbine overall efficiencies, especially at higher operating pressures.

Sealing technology is an area now experiencing increased importance. As the operating pressures have increased in turbomachinery, their tendency to leak has increased since for the same clearance level, a higher pressure ratio leaks more than a lower pressure ratio (until the airflow through the seal becomes choked). Some progress has been made in non-contact seal technology, but it has significantly lagged behind other technological improvements according Wrigley [1]. In the U.S., NASA Lewis Research Center has also pursued experimental evaluations to improve sealing technology, the motive for this research has been reducing fuel consumption of gas turbine engines for the U.S. Military thus reducing operating costs. According to the NASA Lewis report, contained in the AGARD collection of 1978, component efficiencies still have potential for improvement, and much of that improvement could be achieved through advancements in sealing technology. Advanced seals could easily result in a 1/2% efficiency gain for far less cost and risk than a complete redesign of the compressor blades (as described above) [1].

In order to improve sealing technology, a test bed is required to better understand the highly complicated flow through a seal, and to adequately collect data in support of Computer Fluid Dynamics (CFD) simulations. To provide a facility in support of improving sealing technology, this two dimensional planer pressurized air labyrinth seal test rig has been designed. The major goals for this test rig are:

1. To conduct experiments at Reynolds and Mach numbers that are typical of modern gas turbines on large scale, geometrically similar 2D seals.
2. Support accurate bulk flow measurements to verify 2D representations of optimum non-contact seal designs through modification of the number of knives, roughness, orientation, spacing and geometry.

3. Make detailed flow field measurements of sufficient resolution by LDV, hot wire, and pressure transducers to compare with CFD code results.

This report is organized into five main chapters and is followed by a section of figures containing the test rig design drawings and flow prediction graphs. Chapter I provides an introduction, and is followed by Chapter II-Background, which provides a literature review of labyrinth seal research. Chapter III-Design Calculations covers design constraints, desired airflow inlet conditions, test rig preliminary design proposals, and design of each test rig component including the piping system. Chapter III also contains example calculations. Chapter IV-Data Acquisition System covers the proposed computer controlled data collection system and its associated components for which the rig is designed to employ. Chapter V-Test Rig Performance discusses the factors pertaining to labyrinth seal effectiveness and provides a model formulation from which a computer program was written to predict Mach number, Reynolds number, and flow rates for various seal configurations. This chapter also discusses the results of various simulations. Chapter VI-Conclusions and Recommendations describes the overall results of this report and provides recommendations for further areas of study.

II. BACKGROUND

The concept of limiting fluid leakage using a number of restrictors is not a new idea. In his review of Labyrinth Seal literature, Sneek [2] credits C.A. Parsons with development of the labyrinth seal in concert with Parson's [3] development of the steam turbine near the end of the 1800's. As Sneek describes it, Parson's idea was to create a torturous flow path between high and low pressure regions by means of a series of non-contacting restrictors and separating chambers. The main function of the restrictors was to dissipate the kinetic energy of the fluid flow in the separating chambers and thus reduce the leakage from high to low pressure areas. Parson's original method of multiple sealing knives has changed very little except for more modern geometry and orientations.

The first pioneering theoretical paper on labyrinth seal design was introduced by Martin [4] in 1908. Martin considered the labyrinth to be a series of discrete throttling processes very similar to flow through orifices. Martin derived a formula for labyrinth seal leakage based upon a number of simplifying assumptions namely: flow through the seal was isothermal, all knives and cavities were symmetrical, kinetic energy was completely destroyed in each cavity, and the airflow was sub critical (not sonic, i.e., flow not choked). Most researchers following Martin's published work focused on modifying some or most of Martin's original assumptions. Gercke [5] modified Martin's equation with the addition of a kinetic energy carry-over factor. He assumed the flow through the seal was adiabatic in that the flow would return to an isothermal condition via a constant pressure process at each throttling. This theory supported the establishment of his kinetic energy carry-over factor. Gercke also modified Martin's formula for varying areas between the restrictors.

The next major modifier of Martin's formula was Egli [6] in 1935. Egli examined the use of Martin's formula for fewer than 4 restrictors in both incompressible and semi-compressible flows. One of Egli's main contributions was that he noted the pressure ratio across each restrictor increases as the flow moves from the first restrictor to the last.

Therefore the last restrictor is always the first (assuming same gap size through the seal) to choke (reach critical flow pressure ratio). Egli also experimentally determined that the last restrictor would not choke at the same pressure ratio as a sharp edged orifice since its flow coefficient increases as the pressure ratio increases. Egli produced test results for seals showing the effect of gap size and knife thickness on seal performance.

Hodkinson [7] in 1939 was the first to approach the kinetic energy carry-over factor of Gercke from a fluid dynamic standpoint rather than a thermodynamic standpoint. He considered the interaction of the flow encountering the next sealing knife as a jet with portions being sheared off by the obstruction of the knife. Jerie [8] in 1948 examined the effect of the knife thickness to clearance ratio on the seal performance. He determined that when this ratio was greater than 2:1 than the knife behaves similarly to a rounded nozzle instead of a sharp edged orifice. Jerie also determined that a tooth depth to tooth spacing ratio of slightly less than 1 yields an optimum performing seal (minimal leakage). There were some other papers between 1948 and 1961 of minor importance from Kearton and Keh [9] and Zabriske and Sterlicht [10] concerning flow coefficients and friction factors, respectively.

The next major paper was by Vermes [11] in 1961. Vermes combines the efforts of Martin, Gercke, Egli, and Zabriske into one major work. Vermes uses Martin's formula and derives new theoretical and semi-theoretical formulas for computation of the leakage. These formulas correlate within 5% to experimental tests for three types of seals (straight, stepped and combination). Vermes also calculates off design seal performance of the seals from both a theoretical and experimental standpoint. In 1977 Stocker [12], working for NASA Lewis Research Center, investigated the influence of rotation on seal leakage with solid-smooth, abrazeable, and honeycomb lands. He also made experimental measurements of flow leakage for the 2D and 3D cases. His conclusions were that advanced seal designs increase seal effectiveness by over 25% when compared to

conventional stepped seals, and rotational effects produced mixed results with regard to seal leakage depending upon the materials used in constructing the seal.

The AGARD conference of 1978 [1] specifically states that meaningful work in the area of sealing technology has not kept pace with advances in the major gas turbine component assemblies, and that resources need to be dedicated to further work in this area.

Chapter V-Test Rig Performance fully develops the equations for determining the flow through a seal and describes the factors affecting seal leakage, therefore these equations will not be developed here.

III. DESIGN CALCULATIONS

A. CHAPTER OVERVIEW

The test rig design began with first establishing a set of design goals. These goals were used to consider a set of design options and tradeoffs and to guide the establishment of a set of preliminary designs. The preliminary designs led to selection of one "best candidate" design for which a more in-depth stress analysis and cost analysis were performed. After ensuring the design had some promise, a complete stress analysis was conducted and detailed mechanical design produced. Meanwhile, a set of performance predictions was generated to verify the design would achieve the original design set points with a low level of risk (both technical risk and safety).

The sections included in this chapter are Design Goals, Desired Inlet Conditions, Design Methodology, Possible Design Approaches, Air supply, Piping and Valves, and design of the Diffuser, Contraction, Test and Exit sections. The chapter is completed by a discussion of the labyrinth seal, and some design configurations used to modify seal performance.

B. DESIGN GOALS

The first choice to be made was the specific design objectives, i.e., what type of seals did we desire to test (straight, stepped, planer, annular, etc.) and to what extent did we want to test them. In most seals the ratio of gap clearance to rotor diameter is so small the 3D annular seal may be considered 2D planer (Figure 1.1), especially if the rotor rotation is not particularly high and the fluid friction coefficient is low (as is the case with air). With the desire to match gap Reynolds numbers and Mach numbers that occur in real gas turbines (with realistic seal geometry and large scale to facilitate instrumentation) it was decided that an effective 2D planer seal test rig would suffice. The typical Reynolds number range in a gas turbine engine will run to about 10,000 in the compressor and to greater than

100,000 in the turbine, with axial Mach numbers less than 0.9 and pressure ratios of 2 to 3. A 2D annular design (fixed) was considered due to the lack of end wall effects (end wall effects are particular to 2D test rigs due to boundary layer growth along the edges), however the ability to construct a curved view port was in doubt as was the ease of instrumenting the rig (the rig would have to be very large to facilitate instrumentation), this rig would be cost prohibitive. The following major design goals and are listed below:

1. Safety was the overriding concern on this project. Thus a minimum Factor of safety (FOS) of 3 against yield was the design point for each component.
2. A test rig of the smallest size while preserving good aspect ratio and adequate LDV control volume was desired, this resulted in seals scaled upward by about a 10:1 margin.
3. Continuous run operation, the airflow supply was limited by available equipment to 2000 SCFM and 150 psig as shown in Figure 3.1. Blow down operation was considered, however this would impact other users of the air supply system by depleting the reserve air supply and would require recharge intervals (however users of the blow down rig would not significantly affect this rig's operation as it would require no recharge time).
4. Cost and ease of construction were very important, the rig needed to be cost effective and "construction friendly".
5. Once constructed, the test rig required maximum expandability, user friendliness, and low maintenance. This necessitated the development of a modular design.

C. DESIRED INLET CONDITIONS

Gas turbine engine labyrinth seals, although performing the same sealing function in both the compressor and turbine sections, often encounter widely variable conditions of airflow conditions based upon design, operating speed, operating temperature and pressure. In fact, even seals within the same section such as two sets of compressor seals, may experience variable inlet air profiles. With this in mind, it was desired for the test rig to possess some method able to produce an adjustable air entrance profile at the test section thus replicating real engine conditions. The effect of air entrance profiles on seal performance is not well understood, thus it is an important aspect to consider in constructing labyrinth seals.

The rig was thus required to produce flow from smooth and uniform profiles to turbulent linear and non-uniform profiles, with provisions for introducing shear or vortex conditions. A method was also desired to vary pressure ratios from 1.2 to 3.0.

D. METHODOLOGY

To provide the range of profiles described in section C. above, a source of airflow modification methods was required. Although many books on wind tunnels were reviewed, only one particular wind tunnel book by Pope [13] was consulted and its impact on the design of the test rig appears in following sections. The wind tunnel information was utilized to determine the impact of screens, honeycombs, expansions and contractions on modifying the airflow. Using the information from the wind tunnel literature and considering the constraints of part B, 3 designs were considered. These designs were evaluated for structural integrity using simple plate equations for stress and strain and modified as required. A final design was chosen based upon strength, size, ease of construction, and ease of modification. Each of the preliminary designs is discussed in section E.

E. POSSIBLE APPROACHES

Proposal #1 consisted of a diffuser designed for maximum pressure recovery and included both horizontal and vertical transitions of 5-6 degrees with internal splitter vanes. The diffuser was designed in 2 sections, a first diffuser stage followed by a fine screen, then followed by a second diffuser stage ending with multiple fine screens and a honeycomb section. The diffuser was expected to require 35 psig in diffuser assembly and employed a 3D large area ratio (6.7) final contraction section would form the air into a very smooth profile (less than 2% total turbulence). The problem with this design was its complexity, projected construction time, size, cost, and possible problems with separated or highly non-uniform flow.

Proposal #2 was similar to #1 with the exception of a modified diffuser assembly that would now be one piece with separate 2D horizontal and vertical transitions, an 8 degree diffusion angle with many splitter vanes, and a series of diffuser stage screens still ending with 1 honeycomb section. At the diffuser exit would be a smaller contraction ratio (3.3 vice 6.7) operate with 35 psig in the diffuser assembly (still designed for maximum pressure recovery) and maintain a 3D final contraction section. The major problems with this design was complex placement of the numerous vanes, still time consuming to construct, and most importantly the questionable ability to "shear" the gauss distribution of the air inlet into equal parts for effective diffusion. This design would have even more chance of being affected by separated or highly non-uniform flow than proposal #1.

Proposal #3 incorporated a diffuser being of a "dump" type (not designed for maximum pressure recovery) with a removable top plate for easy repositioning of screens and honeycombs according to guidance received by Dr. Hornung [14]. The diffuser would contain only vertical transitions with no vanes, but a series of torturous air paths, multiple diffuser stage screens, and multiple honeycomb sections. Diffuser operating pressure would now be 45 psig due to the increased diffuser losses, this was an increase from 35 psig. The final contraction section changed to only a vertical contraction (Area ratio of 6).

The problems with this design are: it is now very heavy, it must be corrosion protected, and there is no way to correctly predict the airflow profile and initial perforation plate placement. The test section did not change appreciably from the initial design, it is constructed of steel and 1" glass plate. Sensors are mounted either on seal or on top plate (replacing glass), and are discussed more fully in Chapter IV.

F. AIR SUPPLY, PIPING AND VALVES

Air is supplied to the test rig area from a 3 stage 600 Hp Elliot centrifugal air compressor producing 2000 SCFM at 150 psig and 180 °F maximum outlet temperature (Figure 3.1). The air passes through an air drier assembly and to an additional air compressor capable of boosting the exit pressure to 300 psig. In most circumstances the boost pump is bypassed and the air is fed directly into an 8000 ft³ storage tank group that supplies the test rig area. The air is piped into the test rig area through 4 inch diameter stainless steel piping, the connection designed to be utilized by this test rig terminates with a steel blank flange with a standard 6 bolt pattern of 1/2" bolts. Since the supply manifold runs the length of the building and supplies other test rigs, the upstream building shutoff valve can not be used as the sole on/off valve for this test rig since it impacts all air users in the building. Therefore, a dedicated 4" full shut off valve rated to 300 psig is required. The shut off valve can also be used as a throttling valve when the manifold is pressurized to 300 psig (when the 2X boost pump is in operation) to prevent pressures greater than 150 psig in the test rig piping.

A drawing of the pipe connection flange, required to replace the manifold blank flange, is included as Figure 3.3. This flange is designed for minimal flow loss and reduces the 4" manifold diameter to a 2" diameter. To determine the flow loss coefficient for this flange design, tables from White [15] were consulted. Thus for a loss coefficient of 0.005, a required radius/overall diameter = 0.20. Knowing the inlet diameter of the pipe is 1.939", a value of r is determined to be 0.388". The next larger size (using 1/16"

increments) is 7/16" that equals 0.4375". Utilizing the supplied airflow as a guide (2000 SCFM), air mass flow was determined from the following equation:

$$\rho_{std} = \frac{P}{RT} \quad (3-1)$$

$$\rho_{std} = \frac{(14.7 \text{ psia})(14.7 \text{ in. Hg})}{(53.3)(520)} = .076 \frac{\text{lbm}}{\text{ft}^3}$$

$$(.076 \frac{\text{lbm}}{\text{ft}^3})(2000 \frac{\text{ft}^3}{\text{min}}) = 2.55 \frac{\text{lbm}}{\text{sec}}$$

A pipe diameter of 2" was chosen to reduce the cost of the components, and facilitate structural design (smaller structures are less massive for equivalent strength). In the interest of having a smooth pipe wall with minimal upkeep, and simplified pipe connections, the pipe chosen for this rig was 2" schedule 80 PVC rated to 600 psig. The inside diameter of 2" schedule 80 pipe is nominally 1.939". PVC pipe is very temperature sensitive, and loses strength with temperatures much higher than standard conditions. Although the compressor outlet temperature can approach 180 °F, the massive size of the storage tanks (8000 ft³ made of 1.5" steel plate) and long run of piping exterior to the building (approximately 200 feet) allows the air supply manifold temperature to remain below 110 °F, especially with the normal Monterey temperatures around 65 °F. Schedule 80 PVC pipe must be derated by 33% strength at 110 °F (to 400 psig), and 50% (to 300 psig) at 140 °F according to ASTM D-1784.

The valves required for this test rig all must be of the full port design, i.e., the inside air passage diameter must not be less than the pipe internal diameter otherwise the test rig air flow will be reduced and the test rig will fail to achieve designed operating points.

The following valves (or equivalent) should be procured prior to initial construction in order to account for any changes required in connections prior to construction, the valves should be of sturdy construction and rated to 300 psig (shut off and regulator). Fisher series 667-ET stainless steel valves would be a good, but expensive choice:

Name	Size	Type	Notes
Manual-Shut-off valve	2" pipe thread to 2" pipe thread	Globe valve full port	ability to reduce inlet pressure 300 to 150
Adjustable-Pressure Regulator valve	2" pipe thread to 2" pipe thread	Regulator full port	regulate 0 to 45 psig, tight shut off.
Pressure-Relief valve	1" pipe thread	Relief, spring adjustable	ability to set relief range 35-50 psig
Outlet-Control valve	4" flange or 4" pipe	Throttling Butterfly or Globe, full port	max pressure 30 psig

Table 3.1

A filter is included in Figure 3.2, this filter is required since no upstream filtration capability exists within the air supply system. The use of the filter will be required to ensure long life of all fixed sensors, particularly hot wire probes. The filter chosen is a Dollinger coalescing model GP-198-0030-020 rated for 180 psig (maximum) and 840-1008 SCFM at 150 psig with a pressure drop of 2 psig. This filter is advertised to have a 99.9% efficiency at removing .3 micron and larger contaminants (including water and oils). A differential pressure gauge is included with the filter assembly and indicates when the filter media requires changeout. Inlet and outlet connections are 2" NPT.

G. DIFFUSER ASSEMBLY

To facilitate ease of construction, potential modification, and robust design, a rectangular dump diffuser is employed. In order to adjust the air profile exiting the diffuser, a removable bolted top is included (with lifting padeyes). The diffuser can be modified with a number screens, honeycombs, and perforations if desired. The factors governing the application of screens, honeycombs, perforations, and contraction ratios are discussed in section H. Diffuser section drawings are contained in Figures 3.4 to 3.10.

The Diffuser assembly is comprised of a 1" steel bottom plate with 0.75" welded side plates and a 0.75" welded entrance plate. These plates have welded flange connections to secure the removable 1" top plate. Internally the diffuser holds welded sections of 0.25" steel plate of various lengths to act as spacers for the perforation plates, screens, and honeycombs. Allowance is made for two side plates and a bottom plate welded together to form each spacer, the exit section flange is stepped down to secure the last set of spacer plates. The exit of the diffuser section has a bolted connection flange to the contraction section. All bolts used in the diffuser and contraction section are 1/2" diameter SAE grade 1 or above, coarse threaded. The following factors of safety (FOS) exist:

3.3 diffuser front plate (FOS 9.9) with 3X stress concentration factor.

4.42 diffuser top plate

9.9 diffuser side plates

5.75 attachment bolts

In completing stress calculations for the top plate, an expected maximum operating pressure in the diffuser was chosen as 45 psig. The diffuser top plate area subject to this internal air pressure was an area 18" wide and 33" in length. Using Roark's Handbook for Stress and Strain [16] in the case of a rectangular plate with 4 fixed edges (case 8) the following formulas apply:

For maximum stress at the center of the long edge:

$$\sigma = \frac{0.4974qb^2}{t^2} \quad (3-2)$$

For maximum stress at the center of the plate:

$$\sigma = \frac{0.2472qb^2}{t^2} \quad (3-3)$$

For maximum deflection at the center of the plate:

$$y = \frac{0.028qb^4}{Et^3} \quad (3-4)$$

Variables:

$$q = 45 \text{psig}$$

$$b = 18"$$

$$E = 30E6 \text{psi}$$

$$t = \text{thickness}$$

From these formulas, the maximum stress at 45 psig on the 1" top plate is 7246 psi at the edge, 3601 psi at the center, with a maximum center deflection of 0.01". The same formulas are utilized for the surrounding plates to generate stress predictions. To calculate bolt strength, Shigley's Mechanical Engineering Design book [17] was utilized for bolt specifications. Shigley's book contains specific formulas to optimize the use of bolts and fasteners based upon their stiffness, however his method was very time consuming and cumbersome. Through previous experience with these formulas it was determined that by choosing a significant factor of safety (generally 4 or more) against the proof yield strength of the bolts, a very conservative and yet rapid determination of the number of fasteners

could be made. With this in mind, an initial FOS of 5 was chosen, and based upon geometric considerations the resulting number of 1/2" bolts (using the lowest strength SAE grade 1) was determined to be 34, this in turn resulted in the 5.75 FOS.

$$\text{Force on top plate} = (45 \text{ psi})(18")(33") = 26,730 \text{ lbf}$$

$$1/2" \text{ bolt stress area} = 0.142 \text{ in}^2$$

$$\text{Grade 1 yield strength} = 32 \text{ kpsi}$$

$$(0.142 \text{ in}^2)(32 \text{ kpsi}) = 4544 \text{ lbf/bolt}$$

$$\text{so for FOS} = 5, \text{ each bolt can only hold } 909 \text{ lbf}$$

$$\text{therefore \# bolts} = 26730/909 = 29.4 \text{ bolts}$$

Screens and honeycombs are the primary flow conditioners used to modify airflow in the diffuser, and they may be arranged at various positions within the diffuser assembly utilizing 0.25" spacer plates as discussed previously. Although the perforated sections will aid in breaking up the Gaussian air flow profile exiting the inlet pipe to the diffuser, no reliable data exists concerning the best configuration for this task. The preferred location of the 1st perforation plate is even with the inlet tube cap at approximately 5.0" from datum. Datum is the zero point defined as the inlet wall of the diffuser. The perforated inlet pipe attempts to double the area of the mean inlet flow and strain in to the sides of the diffuser. The 1st perforation plate has twice the airflow area of the proceeding perforated section and tries to maintain the flow towards the edges of the diffuser. It is located at the 9.25" datum location. The second perforation plate again doubles the effective flow area and tries to form a somewhat uniform profile flow into the honeycomb section. The second perforated plate is located at 9.5" from datum.

Screens have seen very widespread use both as turbulence reducers (fine wire and spacing far upstream of the test section) and as turbulence enhancers (coarse wire cloth just preceding the test section). Screens typically behave in the relation as set forth by Dryden in 1929 [18]:

$$\frac{U_d'}{U_u'} = \frac{1}{(1+k)^{1/2}} \quad (3-5)$$

where U_d' and U_u' are the root mean square of the velocity fluctuations downstream and upstream of the screen, respectively in x, y, and z directions. The pressure drop factor k, and the number of screens n are also variables. As an example problem, if 2 screens are used and each screen is comprised of 18 mesh wire of 0.011" diameter wire with a k=0.842 at a velocity of 20 feet/second, the turbulence will be reduced by 46.7%.

A concern when utilizing screens is the drag on the mesh due to the airflow. In the above case the drag/ft² =kq, where q is the mass flow/ft², the drag is 0.4lb/ft² and for a screen of 9"X18" the total drag would be only 1.13 lbf on the screen. The recommended screens for the test rig should be constructed of 20 mesh 0.017" wire diameter (with K=1.8) screen located at the 20", 24", and 28" points from diffuser datum. This spacing will allow adequate mixing and evening out of the flow between the screens. These screens should yield a turbulence reduction of 78.7% using Equation 3-5.

Honeycombs are primarily used to strain the flow and make it close to 1D as possible by breaking up large scale structures. The honeycomb prevents circulation and lateral velocity variations from propagating as the flow progresses. The only real rules of thumb for the honeycomb, is that the length of the honeycomb should be 5 to 10 times its cell diameter, and the octagon configuration typically yields the lowest pressure drops compared to circular or square patterns. The recommended honeycomb is 0.25" diameter hexagons of aluminum construction of 2.5" in length. The honeycomb leading edge should be located at the 13.5" datum location and secured by press fitting into place and placing

0.25" spacer plates upstream and downstream of this location. Wall interfaces should be sealed by the use of a flexible RTV or Permatex to prevent errant flow around the honeycomb.

H. CONTRACTION SECTION

The contraction ratio of any test rig, or wind tunnel, is an important item to consider for two reasons: 1) the desired contraction ratio will determine the size of the diffuser and test sections, and 2) the contraction ratio has a major effect on the longitudinal velocity variations within the flow path. As discussed by Pope [13], a properly chosen contraction ratio has a major contribution to improving the performance of a wind tunnel/test rig. To determine the effect of contraction ratio some background is required in accordance with Pope's discussion.

v_u =upstream velocity variation

v_d =velocity variation after the contraction

V_u =upstream mean velocity

V_d =mean velocity after the contraction

n =contraction ratio

Writing Bernoulli's equation assuming pressure and gravity loss is negligible

$$\frac{1}{2}\rho(V_u + v_u)^2 = \frac{1}{2}\rho(V_d + v_d)^2 \quad (3-6)$$

$$v_u^2 + 2v_u V_u = v_d^2 + 2v_d V_d \quad (3-7)$$

Dividing by V_u^2 / V_d^2 and neglecting the $(v/V)^2$ term as being very small

$$\frac{v_d}{V_d} = \frac{V_u^2}{V_d^2} \frac{v_u}{V_u} \quad (3-8)$$

$$V_u^2 / V_d^2 = 1 / n^2 \quad (3-9)$$

$$\frac{v_d}{V_d} = \frac{1}{n^2} \frac{v_u}{V_u} \quad (3-10)$$

Therefore, the variation ratio of upstream velocities are variable through the inverse of the square of the contraction ratio. For a contraction ratio of 6, the mean velocity variations would be reduced to 1/36 of their initial value, or yield a 97.2% reduction. The contraction section profile was chosen from Pope's book on Wind Tunnel Design [13]. Pope also recommends the contraction cone be led by a settling chamber equal to 0.5 of the equivalent air chamber diameter, and followed by settling chamber of the same size just prior to the test section. A high quality inside contraction profile graph is included with coordinates as Figure 3.12, this figure should be used to shape the contraction curvature with a 9.0" distance between top and bottom plates at the inlet and a distance of 1.5" between the same plates at the outlet.

I. SETTLING/MODIFICATION SECTION

This portion of the test rig allows the air to "rest" and restabilize after contracting in accordance with Pope's discussion in [13]. For this size of airflow area (1.5"X18") an effective length of 2.94" is recommended. The actual settling camber available length is 5" with an additional 1" provided prior to the test section view area. This 3" of available space can be used to generate specific profiles as desired by the user. Some specific recommended flow patterns and how they can be generated are:

1. Shear profile - achieved by placing a fine screen covering only a portion of the airflow area and leaving the remaining area free from obstructions.

2. Vortex profile - using a series of partial span winglets to generate any number of wingtip vortices (generating axial vortex cores).
3. Turbulent profile - achieved through the insertion of a series of trip wires to create vortex shedding and turbulence, or turbulence generated by the injection of air normal to the flow path.

Example drawings of each profile is contained in Appendix C: Flow Modifications. The above recommendations are only a few of the many different profiles which could be achieved not only through modification of flow in the settling section, but by modification of the flow pattern upstream in the diffuser and contraction sections.

J. TEST SECTION

The test section is comprised of four major components, two symmetric side plates, a bottom plate, and a top plate each bolted to one another and bolted to the settling and exit sections. The side plates can be either machined or welded out of 0.5" steel plate, along with the top and bottom plates. The recommended construction technique for the side plates however, is machining out of 1.5" mild steel, with the bottom and top plates being of welded construction. The test section allows for designed gaps of 0.15" with seals 6" long and 18" wide. The test section is designed to be positive locking with no adjustment of the seal once installed, the seal will be bolted into place from underneath the bottom section. Three glass top plates allows the use of a traversing LDV system to measure flow fields from full front to back of the seal an virtually all area covering the width of the seal. Each glass plate is 1 " thick with top dimensions of 6"X4", and bottom dimensions of 5.5"X4", the front and rear surfaces of the plate are beveled to support placement of the plates in the test section top plate. Each glass plate should be protected from direct glass to metal contact by the insertion of thin sealing gaskets or putty. Removal of the top plate assembly for

cleaning or access to the interior of the test section will be accomplished by removing the twenty-two 0.375" bolts. While the top plate is removed the glass plates should be adjusted to give a smooth surface from the front to back of the top plate. Some form of filler (RTV) should be used to fill the small gaps between the glass and steel plates. The experimental seal is constructed of steel to ensure robustness of the edges and corners. It can be made in 1 piece, or multiple pieces depending on the desires of the user. The seal is secured by drilling six 0.025" holes in the bottom plate and passing bolts through the bottom plate into the seal that itself has been drilled and tapped. Additional holes for the passage of instrumentation should be avoided without additional stress factor calculations. Instrumentation cables should be passed through to the exit section where they should exit the rig at one of the 1" back pressure holes and be sealed. Details of the test section design are contained in Figures 3.14 to 3.16. The following factors of safety (FOS) exist:

- 9.9 Flanges inlet and exit
- 3.8 Bottom plate
- 6.2 Each plate glass
- 3.5 Top plate steel
- 12.5 Side plates
- 6.75 3/8" attachment bolts

K. EXIT SECTION

The exit section is designed to minimize back pressure when exit to atmospheric conditions is desired, yet allow back pressure to 30 psig as required for experimentation. Details of this design are included as Figures 3.17 and 3.18. For operation with minimal back pressure, 4 additional 1" diameter tapped holes are provided to vent internal pressure if required and to allow passage of the seal instrumentation cables. These holes will be plugged for normal operations.

IV. DATA ACQUISITION SYSTEM

A. ACQUISITION SYSTEM OVERVIEW

To effectively collect, process, store and display large amounts of data from multiple sensors an automated data acquisition system was required. NPS has recently obtained a number of IBM-PC compatible DATASTOR 486-DX computers with 14" color monitors containing 16 megabytes of random access memory and 535 megabyte hard drives. These computers have full tower cases and six free expansion slots. The school also has numerous National Instruments AT MIO-16F-5 Multi-function I/O boards, IEEE 488 General Purpose Interface Bus (GPIB) boards, and SC2070 GPIB termination breadboards. The computers are configured with Microsoft Windows V3.1 and run Labview for Windows software. Labview is a full featured graphical programming system for data acquisition and control, data analysis, and data presentation. Labview is easily programmed to accept inputs from plug-in boards and supports numerous data collection options beyond the scope of this discussion. This basic system will be interfaced with Scanivalve Corporation self-calibrating fixed temperature and pressure transducers to provide basic data collection as described in the following sections. This will provide an excellent data collection/analysis system. A schematic diagram of the system is included as Figure 4.1.

B. AIRFLOW MEASUREMENT

To accurately measure the flow through the test rig, a provision for a replaceable orifice plate has been made. Orifice units typically contain both upstream and downstream pressure taps and utilize a calibrated sonic orifice plates. The plates are replaceable to maintain accurate flow measurement through the pressure range of the test rig. Orifice plates should generally be chosen to provide less than 1% deviation in the intended realm of rig operation pressures. The upstream and downstream pipe connections for the orifice

assembly are 2" NPT of 1.939" inner diameter on this test rig. The orifice assembly is designed to be mounted just downstream of the pressure regulator valve, and just prior to the entrance of the diffuser assembly. In this position the orifice assembly should experience pressure less than 50 psig; however, a potential drawback to this location is the high pressure drop induced in the orifice which may prevent the test section from achieving the desired pressure and flow rate. An alternative position is to mount the orifice assembly upstream of the pressure regulator (150 psig side), in this position the orifice may be slightly less accurate due to the larger operating pressures, but will guarantee sufficient air inlet to the pressure regulator and test section. The diffuser assembly and pressure regulator threaded connections can therefore be easily switched to allow placement of the orifice assembly at the location desired while preserving sufficient upstream and downstream pipe lengths to yield good orifice results. A straight pipe length of at least 39" should precede the orifice assembly for a fully developed turbulent air profile to occur, and a trailing straight pipe length of at least 12" downstream of the orifice. Channels 1A&B through 4A&B for both temperature and pressure are dedicated to collecting this data.

C. FIXED SENSORS

To determine the condition of the air at any point in the test rig, a series of pressure taps and thermocouples and a traversing hot wire are employed. Two computer expansion slots are filled with SDIU MK5 digital cards, with each card connected to its associated scanivalve. Although the scanivalves are driven by the same drive system, one 48 channel valve set-up is configured for pressure measurements (channel A), while the other is configured for temperature measurements (channel B). Channels 5A through 8B are dedicated to the diffuser section, channels 47A&B and 48A&B to the exit section, and the remaining 38A&B channels to the test section. A major design deficiency of the test rig is its current inability to support rapid repositioning of the sensors while the unit is in operation (however, most test rigs do not have this ability). In fact, no repositioning is

currently possible without partial disassembly of the test rig. Sensors can be mounted at the discretion of the user depending upon the goal of the experiment, but a recommended layout is shown in Figure 4.1. In the recommended layout, the left side of the test rig contains more in-line sensors than the right side, this will allow the user to determine if any ill effects occur due to this placement. Every data location is also supported by at least one and sometimes two redundant sensors. These redundant sensors should also ensure adequate safety monitoring capability. The scanivalve system is self calibrating and has an advertised accuracy of less than 0.1% of full scale.

A DANTEC traversing hot wire system is also recommended to aid in determining flow fields, and as a supplemental mass flow indicator. This system requires two computer slots, one for a GPIB timing board, the other for an AT MIO-16F Analog to Digital board. A calibration unit is provided to facilitate easy verification of data. This system is software controlled and is fully position able through remote means in three dimensions. The results of using the hot wire should be compared with the LDV system described in part C. Accuracy is advertised as less than 0.1% of full scale.

D. NON-INTRUSIVE LDV MEASUREMENT

Many methods exist for determining the state of a flow field, three of them are hot wires, pitot probes/pressure taps, and Laser Doppler Velocimeters. Of the three only one, a traversing LDV, can generate high accuracy data exterior to the test rig. The NPS's recent acquisition of a dedicated LDV system complete with seeding atomizer promises to yield significant results when used in concert with the NPS high speed and low speed test rigs. This LDV system is a DANTEC system with an Enhanced Burst Spectral Analyzer, 3 watt output water cooled laser, and a stand alone data acquisition system. Software is provided by the manufacturer to collect, display, analyze, and modify the LDV data.

The LDV works on the principle of Doppler shifting to determine the 1D velocity of the flow field. The laser beam is produced, then separated into multiple colored beams

(typically split by a prism with the two strongest beams of blue and green collected at the output). Each of these beams are then split again, with $1/2$ of the beam frequency shifted slightly out of phase. Each beam is then focused into the control volume and scattered by the motion of the flow field, sometimes seeding material is required to aid in scattering of the beams. The beams are then collected in either a forward scatter or back scatter mode and analyzed to determine the resulting frequency shifts. Forward scatter is typically the better mode when possible, but the test rig will be limited to back scatter operation only. These frequency shifts are then converted into velocities and collected to obtain a velocity flow field.

V. PREDICTED TEST RIG PERFORMANCE

A. EQUATION DEVELOPMENT

To accurately predict the leakage rates for a given labyrinth seal geometry, and to predict Mach numbers and Reynolds numbers, a method was required to effectively predict flow rates over large variations in seal geometry and inlet pressures. In order to accomplish this, a program was written in MATLAB (appendix A) to satisfy these requirements. Section B discusses reduction of the data into Mach and Reynolds numbers, and the specific program predictions. In order to develop the flow prediction program certain assumptions and simplifications were required:

1. All inlet and outlet conditions of the air are constant, known quantities.
2. The working fluid (air) is a perfect gas.
3. Flow through the seal is adiabatic.
4. The air flow behaves in a semi-compressible fashion at speeds below Mach 0.9.
(i.e. the calculated air density is the average of the inlet and exit air densities across the seal)
5. All jet kinetic energy is dissipated at each intermediate seal cavity.
6. The kinetic energy carryover factor (β) and vena-contracta modification (C_C) are constant for each knife ($\mu=C_C\beta=0.65$).

And although not necessary, the program is written with two fixed parameters:

1. The spacing between the sealing knives are constant.
2. The gap clearance of each knife is constant.

The simultaneous flow equations for both ideal incompressible and ideal semi-compressible flow will be developed for one sealing knife. Utilizing the mass flow equation for 1D steady flow:

$$\dot{m} = \rho A V \quad (5-1)$$

and the equation for the density of air:

$$\rho = \frac{P}{RT} \quad (5-2)$$

and the Bernoulli equation neglecting changes in height, with work terms set to zero, and treating the inlet velocity is zero due to a sufficiently large reservoir (denoting conditions upstream of the first knife by the subscript "u" and conditions at the downstream exit by "d"):

$$P_u = P_d + \frac{1}{2} \rho V_d^2 \quad (5-3)$$

By rewriting terms Equation (5-3) becomes:

$$V_d = \sqrt{\frac{2(P_u - P_d)}{\rho}} \quad (5-4)$$

Combining equations (5-4) and (5-2) into Equation (5-1) an equation for the mass flow through the seal is obtained:

$$\dot{m} = A \sqrt{\frac{2P_u(P_u - P_d)}{RT}} \quad (5-5)$$

To calculate the semi-compressible flow across one sealing knife some modifications to Equations (5-1) through (5-5) will result. Utilizing the mass flow equation (where the "*" represents an average of the upstream and downstream conditions):

$$m^* = \rho^* A V^* \quad (5-6)$$

and the equation for the density of air (assuming the air density is now based on the average pressure across the seal):

$$\rho^* = \frac{P^*}{RT} \quad (5-7)$$

By rewriting terms of the Bernoulli equation using the "*" values while still denoting conditions upstream of the first knife by the subscript "u" and conditions at the downstream exit by "d" Equation (5-3) becomes:

$$V_d^* = \sqrt{\frac{2(P_u - P_d)}{\rho^*}} \quad (5-8)$$

Combining Equations (5-6) and (5-7) into Equation (5-8) an equation for the semi-compressible mass flow through the seal is obtained:

$$m^* = A \sqrt{\frac{(P_u - P_d)(P_u + P_d)}{RT}} = \frac{A}{\sqrt{RT}} (P_u^2 - P_d^2)^{.5} \quad (5-9)$$

The ideal equation (5-9) must now be modified by a flow coefficient μ , which is the actual flow through the seal divided by the ideal mass flow.

An expression for μ is the product of the contraction coefficient C_c (which is the ratio of the minimum jet flow area occurring at the vena-contracta to the minimum area of the orifice) and the kinetic energy carry-over factor, β in [17]:

$$\mu = C_c \beta \quad (5-10)$$

The theoretical value of C_c is 0.611, but has been experimentally determined to be 0.65 for a sharp edged orifice by Lamb [19]. An empirical relation for β based upon seal geometry has been determined by Vermes [11] as:

$$\beta = \frac{1}{(1 - \alpha)^5} \quad (5-11)$$

$$\alpha = \frac{8.52}{\frac{l}{\delta} + 7.23} \quad (5-12)$$

where l is the distance between seals, and δ is the gap between the top of the knife and the stator with both surfaces static.

In combining Equation (5-9) with (5-10) a modified flow rate equation can now be represented with q as the mass flow per unit width of the seal.

$$q = \frac{\delta \mu}{\sqrt{RT}} (P_u^2 - P_d^2)^{.5} \quad (5-13)$$

In reality, the μ modification should be 0.65 for the first knife since no kinetic carry-over exists, with the product of 0.65 and β for the remaining knives. To simplify equation development and MATLAB programming, a constant value of 0.65 is used for all values

of μ although the program does calculate and display a "correct" value for μ based upon Equations (5-11) and (5-12).

As displayed in Figure 5.1 (a four knife seal), Equation (5-13) can be modified for each seal using the upstream and downstream pressures. When setting each q equation equal to one-another and canceling the common terms (R, T, μ , and δ) the following relationship is achieved.

$$(P_u^2 - P_1^2) = (P_1^2 - P_2^2) = (P_2^2 - P_3^2) = (P_3^2 - P_d^2) \quad (5-14)$$

Equation (5-14) can now be rewritten into equations for P_1 , P_2 , and P_3 in terms of only P_u and P_d :

$$P_1 = \sqrt{\frac{3P_u^2}{4} + \frac{P_d^2}{4}} \quad (5-15)$$

$$P_2 = \sqrt{\frac{P_u^2}{2} + \frac{P_d^2}{2}} \quad (5-16)$$

$$P_3 = \sqrt{\frac{P_u^2}{4} + \frac{3P_d^2}{4}} \quad (5-17)$$

Similar relationships can now be determined for N sealing knives. Since the pressure ratios across each knife can now be determined, the use of the compressible flow equation for isentropic flow from White [15] reveals the Mach number across each seal:

$$Ma = \sqrt{5\left(\left(\frac{P_i}{P_{i+1}}\right)^{\frac{2}{\gamma}} - 1\right)} \quad (5-18)$$

Using the relationship $Ma = V/a$, where $a = (\gamma RT)^{.5}$ ($\gamma = 1.4$ for air), the velocity of the air flow through each knife can be determined.

Reynolds numbers can be determined by using the gap δ , the velocity V , and kinematic viscosity of air ν (with ν averaged for the pressure variations across the seal) according to the formula.

$$Re = \frac{\rho VL}{\mu} = \frac{V\delta}{\nu} \quad (5-19)$$

B. PERFORMANCE PREDICTIONS

The test rig is designed to operate with inlet pressures as high as 45 psia and outlet pressures between 15 psia and 35 psia with seals of 2 to 5 knives and Mach numbers below 0.9. The program in Appendix A was validated by several methods for absolute pressure ratios to 5 (with atmospheric pressure exit), and for seals with between 2 and 14 knives. First, the generated mass flow rates at the inlet, outlet and across each knife were checked to ensure consistency (they agree to 8 decimal places). Second, intermediate pressures were reviewed and Mach numbers checked to ensure increasing Mach numbers towards the downstream seals. Third, the program was run and the output compared with the curves generated by the well known Martin's seal formula [4] (modified by the flow coefficient $\mu=0.65$), in which the generated curves were virtually exact. Fourth, the program was run for a gap clearance of 0.040 inches and 5 knives and the flow rate verses pressure ratio plotted. This graph was compared to a graph previously generated by Vermes' [11] in his work comparing a modified version of Martins formula to experimentally derived data. Again, the MATLAB program and Martin's formula were virtually exact and correlated extremely well to Verme's experimental data (Figure 5.2). The MATLAB program was again run for a seal with 14 knives and a pressure ratio of 5 to determine the intermediate chamber pressures within the seal. These were plotted on the graph of pressure ratio verses scaling knife number and compared with a prior graph of experimental data (again a product of Vermes' work) [11]. The MATLAB program

predicted slightly lower chamber pressures than the experimental results and hence a lower rate of seal leakage (which is to be expected due to the assumptions written into the program), but the predicted curve differed from the measured curve by only 3% to 5% (Figure 5.3).

Confident that the MATLAB program is reasonably accurate to within 5%, Reynolds number and Mach number verses pressure ratio curves were generated for 2, 3, 4, and 5 knife seals each with gaps of 1/32", 2/32", 3/32", 4/32", 5/32". A series of four graphs were produced with exit pressures of 5 psia, 15 psia, 25 psia, and 35 psia (Figures 5.4, 5.5, 5.6, and 5.7 respectively). Figure 5.8 is actually Figure 5.4 displaying only the maximum and minimum Reynolds number and Mach number ranges. Figure 5.9 displays low speed predictions (pressure ratios less than 1.2) for an exit pressure of 15 psia.

Figure 5.10 shows the effect of varying back pressure on the de-coupling of Reynolds numbers and Mach numbers. Thus for a given Mach number, a variation in Reynolds number can be obtained by adjustment of the test rig outlet control valve to produce a back pressure (above atmospheric pressure) on the exit side of the seal. Conversely, if an attachment were connected at the exit to the test section capable of drawing a vacuum, the Reynolds number range could be further increased.

In summary, based on Figure 5.8, the test section should operate with satisfaction below Mach 0.9 with Reynolds numbers up to 100,000. Figures 5.11 through 5.14 display the intermediate chamber pressures and seal leakage rates for 2,3,4, and 5 sealing knives as a function of pressure ratio (to 3) and atmospheric exit pressure. Those figures graphically show that Mach number is always highest across the last seal since the highest pressure ratio exists at that point, independent of the number of knives utilized.

VI. CONCLUSIONS AND RECOMMENDATIONS

A. CONCLUSIONS

This thesis has presented a design of a test facility to aid in improving sealing technology. Based upon the school's available facilities and the level of research desired to be conducted a list of goals was presented driving the design of the test rig. The methodology of design and supporting calculations were presented along with detailed mechanical drawings to support construction of such a test rig. A proposed data acquisition system was presented to allow adequate collection of data, and initial operational procedures for the rig were included. An overview of the factors impacting labyrinth seal performance were presented along with a computer model to predict test rig operating parameters. Graphs of the test rig operating realms were produced along with a required test rig parts listing. The overall conclusions are:

1. The 2D test rig design will be cost effective, simple to construct, and provide projected performance.
2. The proposed design met the design goal of operating with a factor of safety greater than 3.3 at conditions of $Re_{gap} \leq 100,000$ and $Mach \leq 0.9$, to match Reynolds and Mach numbers that occur in real gas turbines, and to support measurements of significant resolution for CFD validation.
4. Modification of the diffuser assembly may be necessary due to the lack of information concerning dump-diffusers, and the uncertainty associated with perforation plate, screen, and honeycomb locations.

B. RECOMMENDATIONS

The primary recommendation based upon this thesis is to build a 2D test rig according to the provided specifications. Once constructed the test rig should be used to validate the MATLAB program flow rate and chamber pressure predictions by experimental research, and eventually modify the MATLAB program for variable carry-over factors and irregular knife gap and spacing. The rig should then be used to optimize labyrinth seal design. After the basic operation of the rig has been substantiated, further modifications of the rig should be considered to improve performance as follows:

1. Consider an eductor system to create a vacuum at the seal exit, this would provide additional range for both the available Reynolds number and Mach number without raising the internal operating pressure of the system.
2. Consider perforations and suction on the end walls to minimize boundary layer growth and the subsequent "end wall effect".
3. Design and construct a 3D rotational test rig to determine the effects of rotation on seal performance specifically, this rig could be used for measurements of flow coefficients, friction factors, and heat transfer.
4. Design and construct a modified test section to allow testing of staggered labyrinth seals.

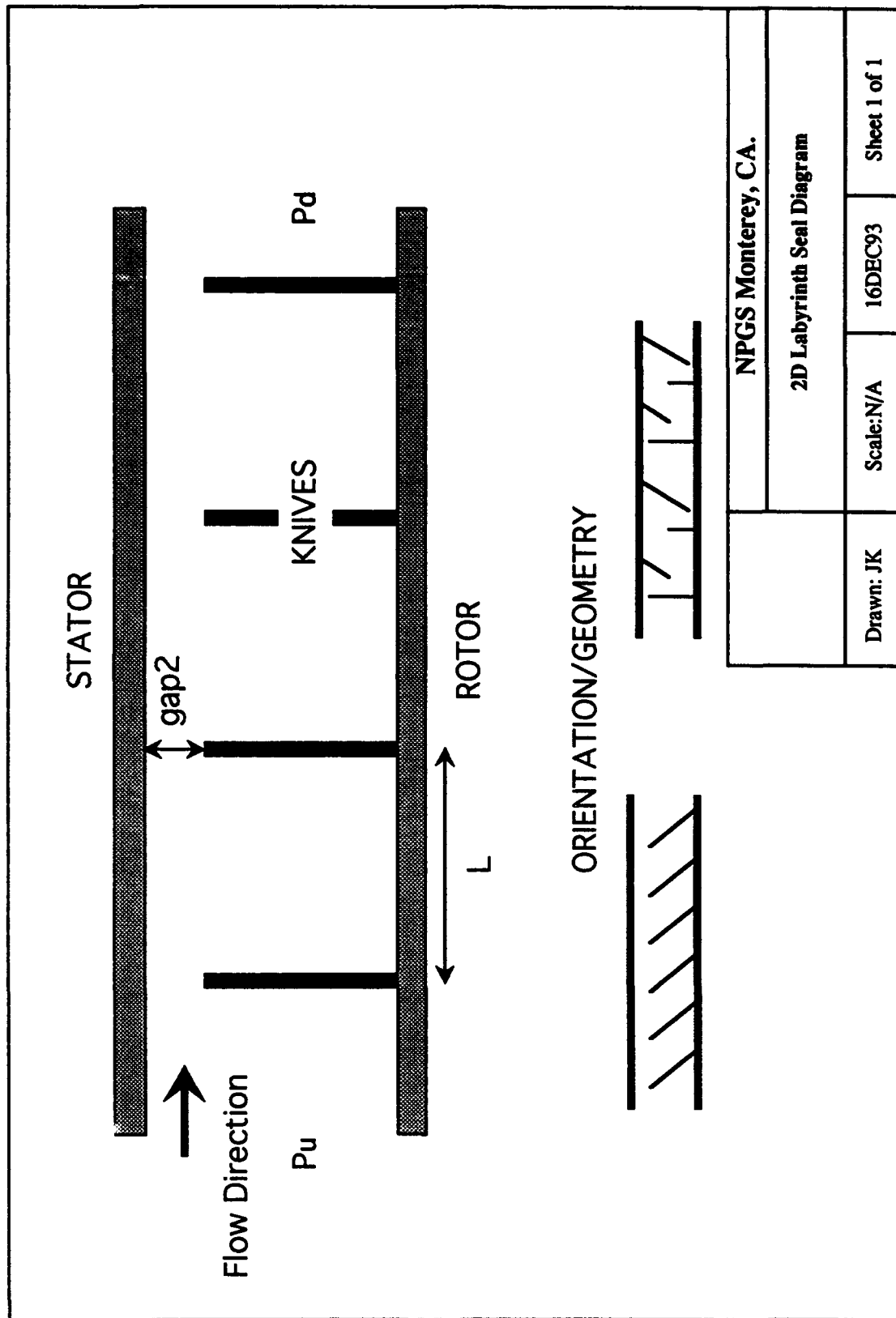


Figure 1.1 Labyrinth Seal Diagram

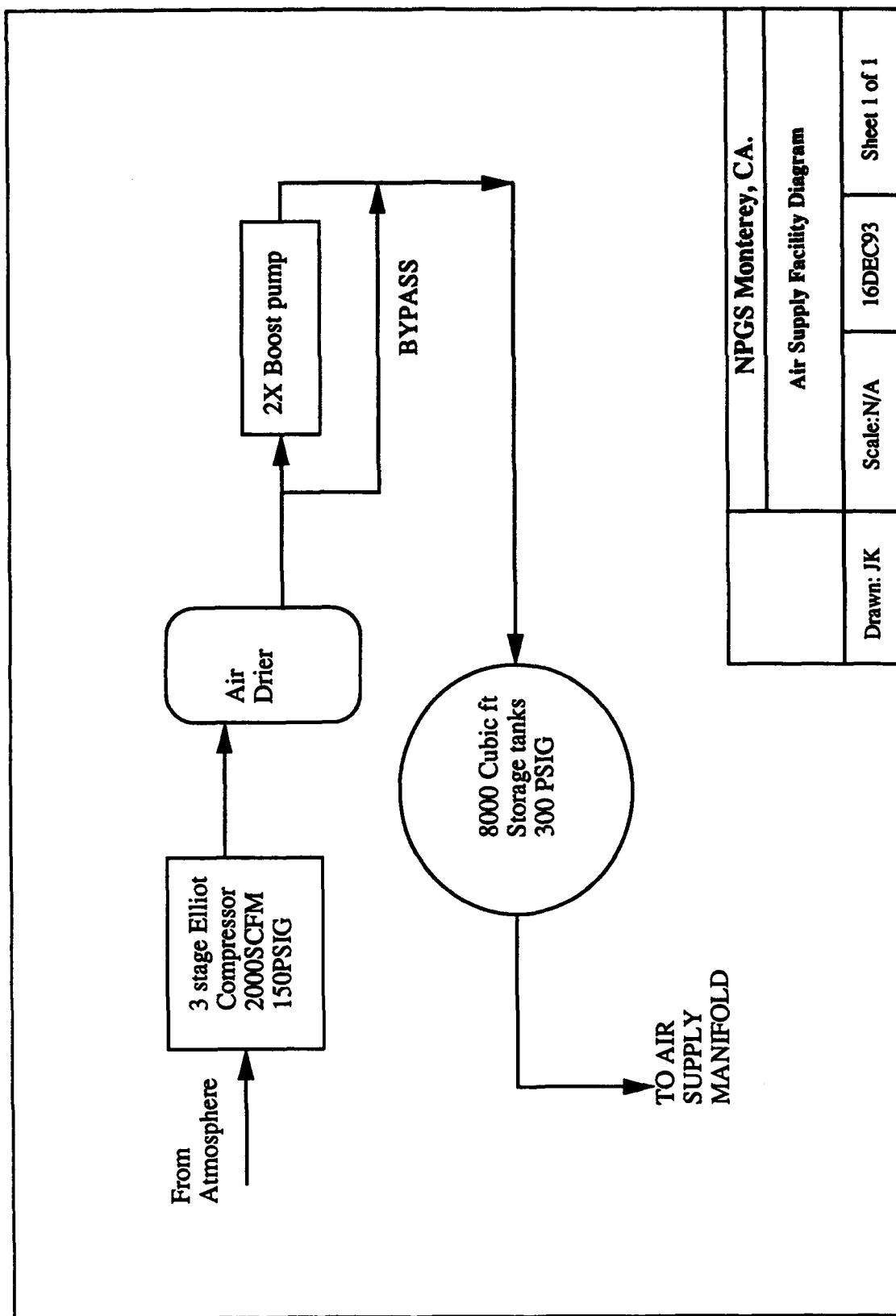


Figure 3.1 Air Supply Facility Diagram

2D Labyrinth Seal Test Rig Schematic with Dump Diffuser and 2D Contraction

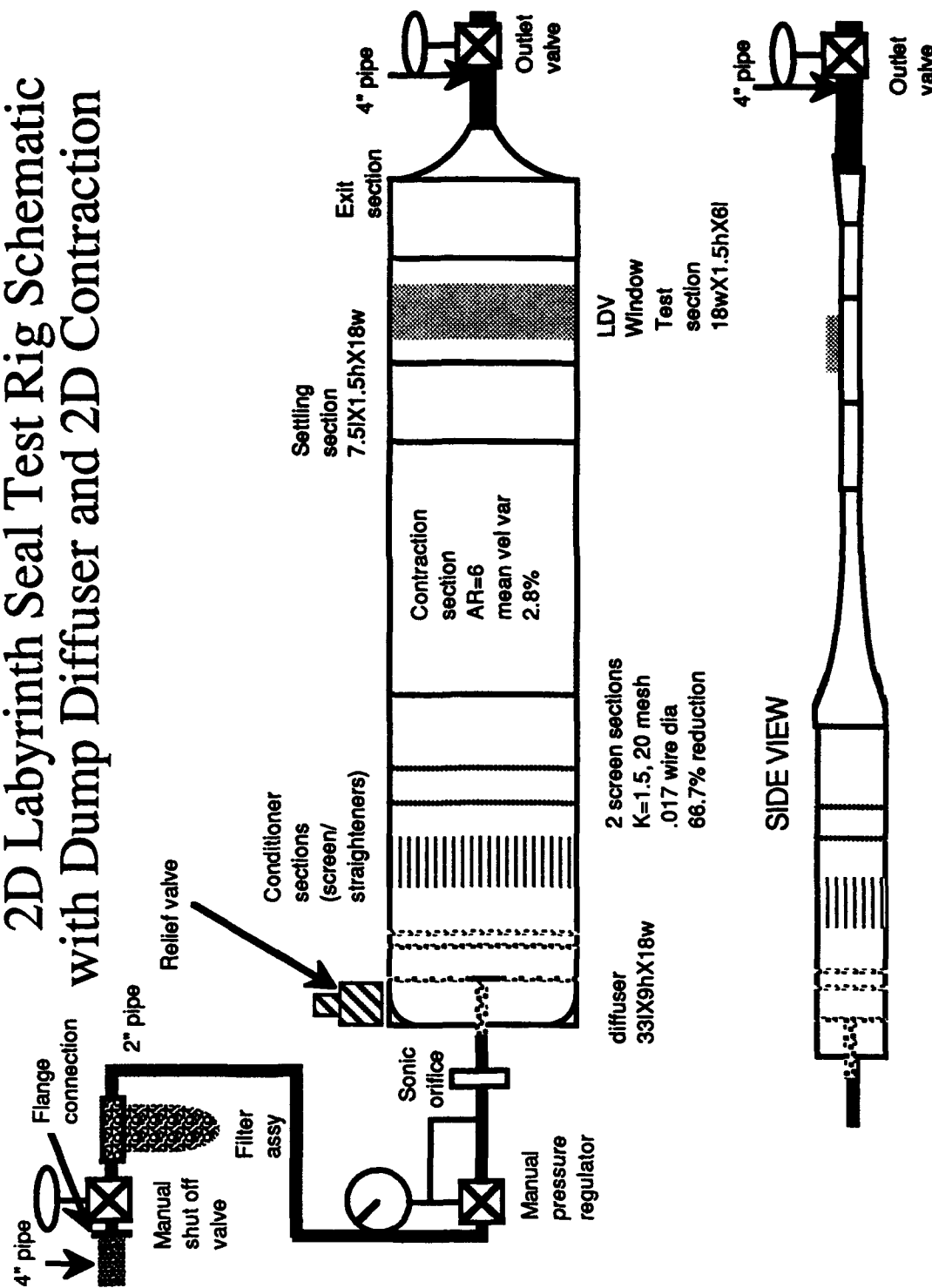


Figure 3.2 Test Rig Schematic

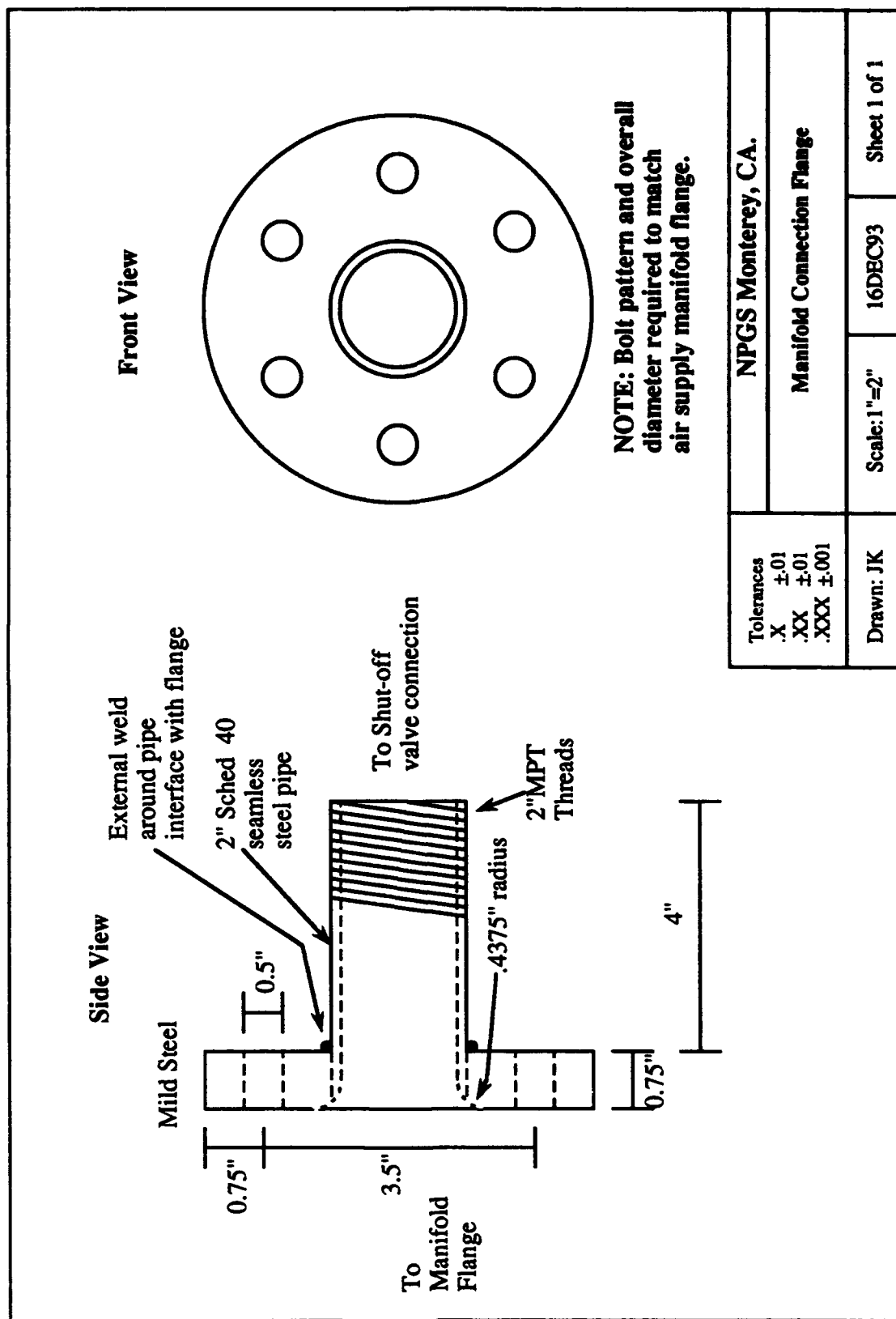


Figure 3.3 Manifold Connection Flange

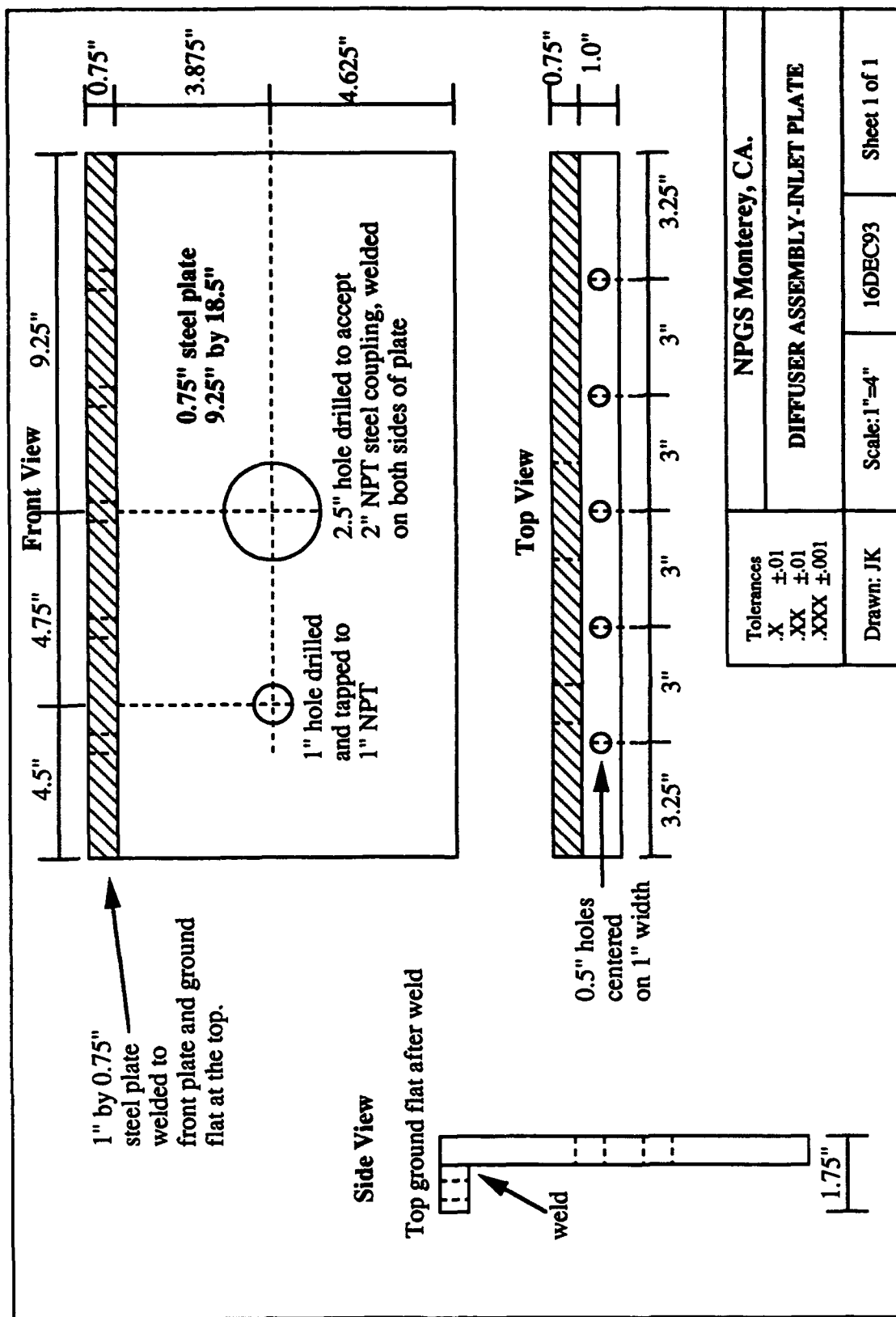


Figure 3.4 Diffuser Assembly Inlet Plate

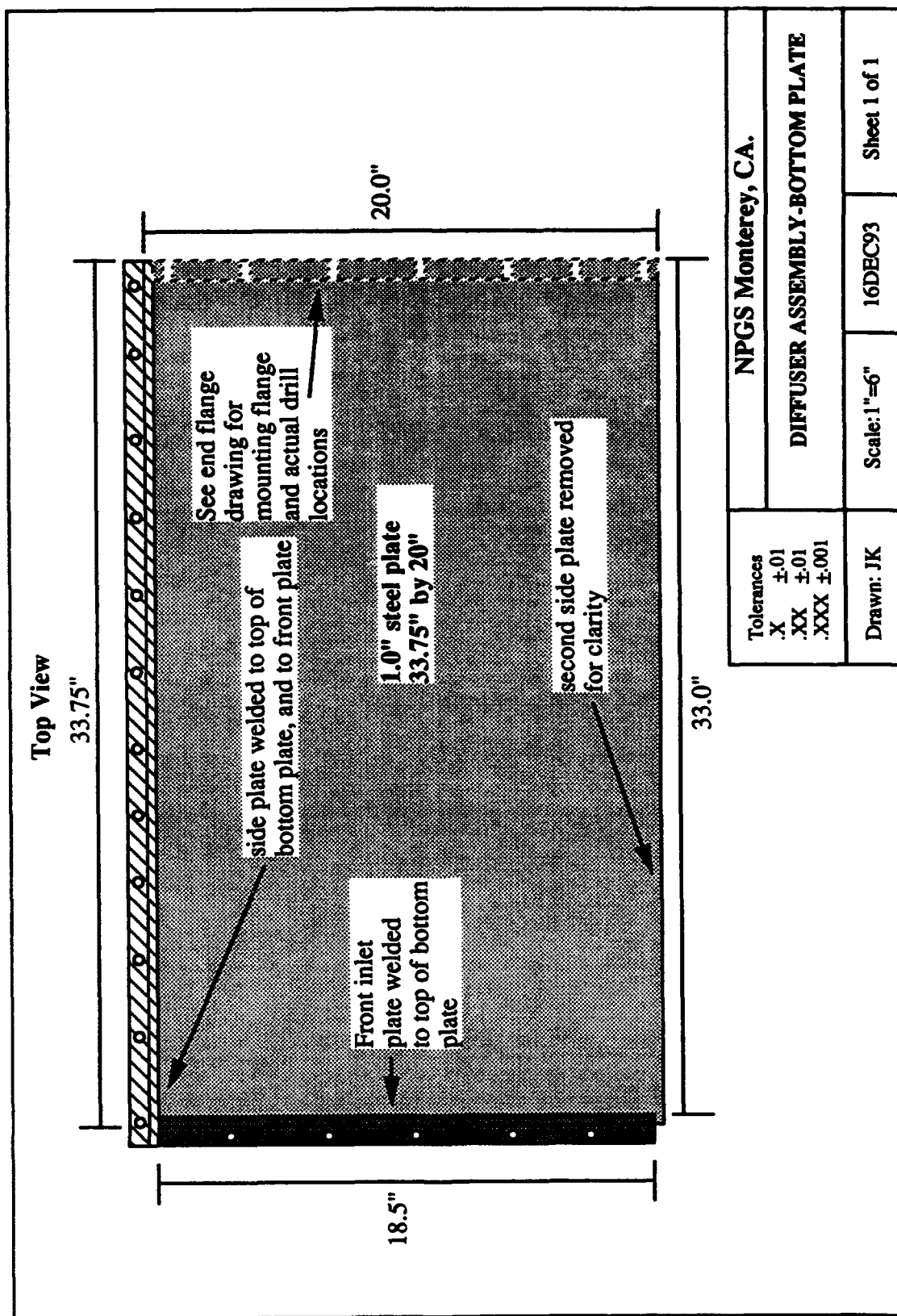


Figure 3.5 Diffuser Assembly Bottom Plate

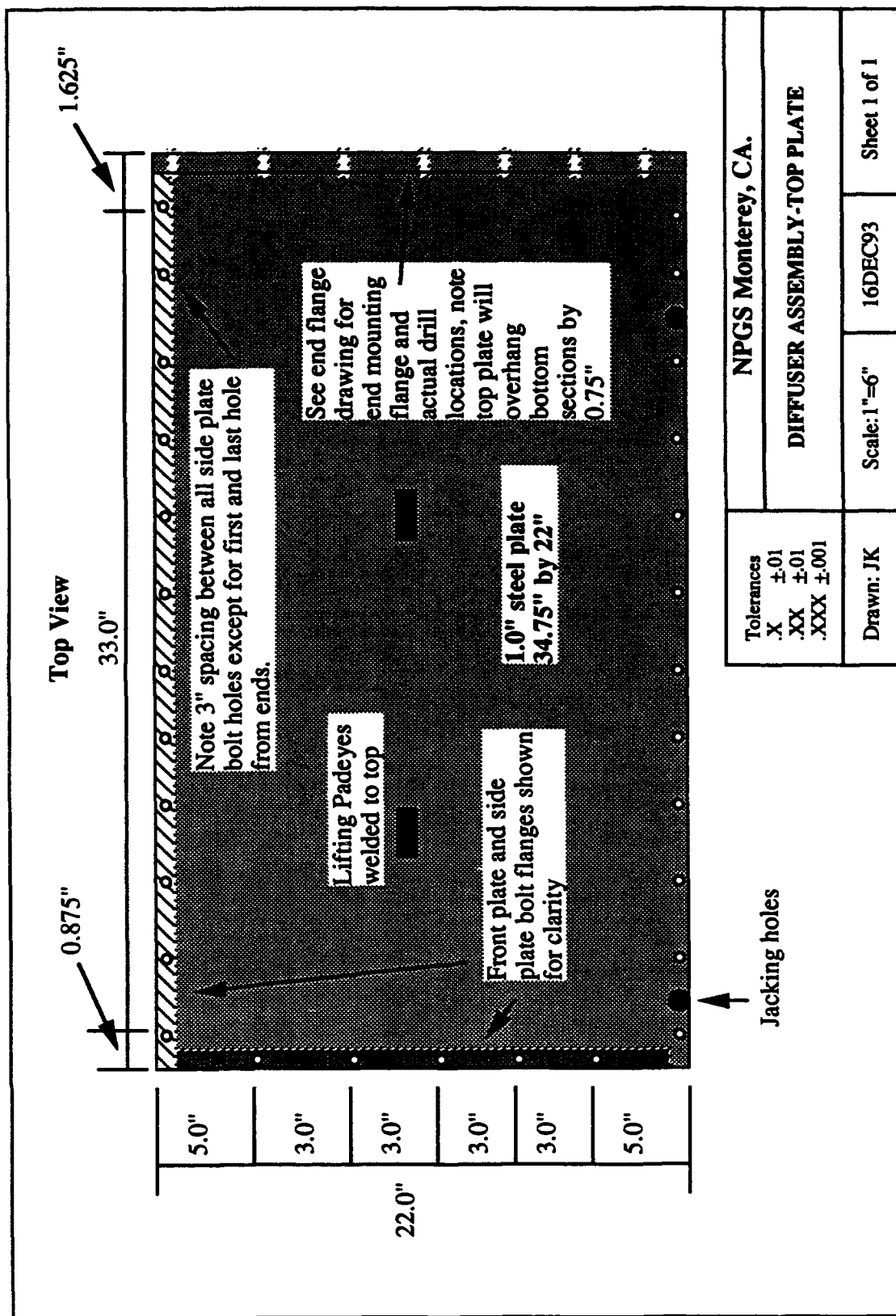


Figure 3.6 Diffuser Assembly Top Plate

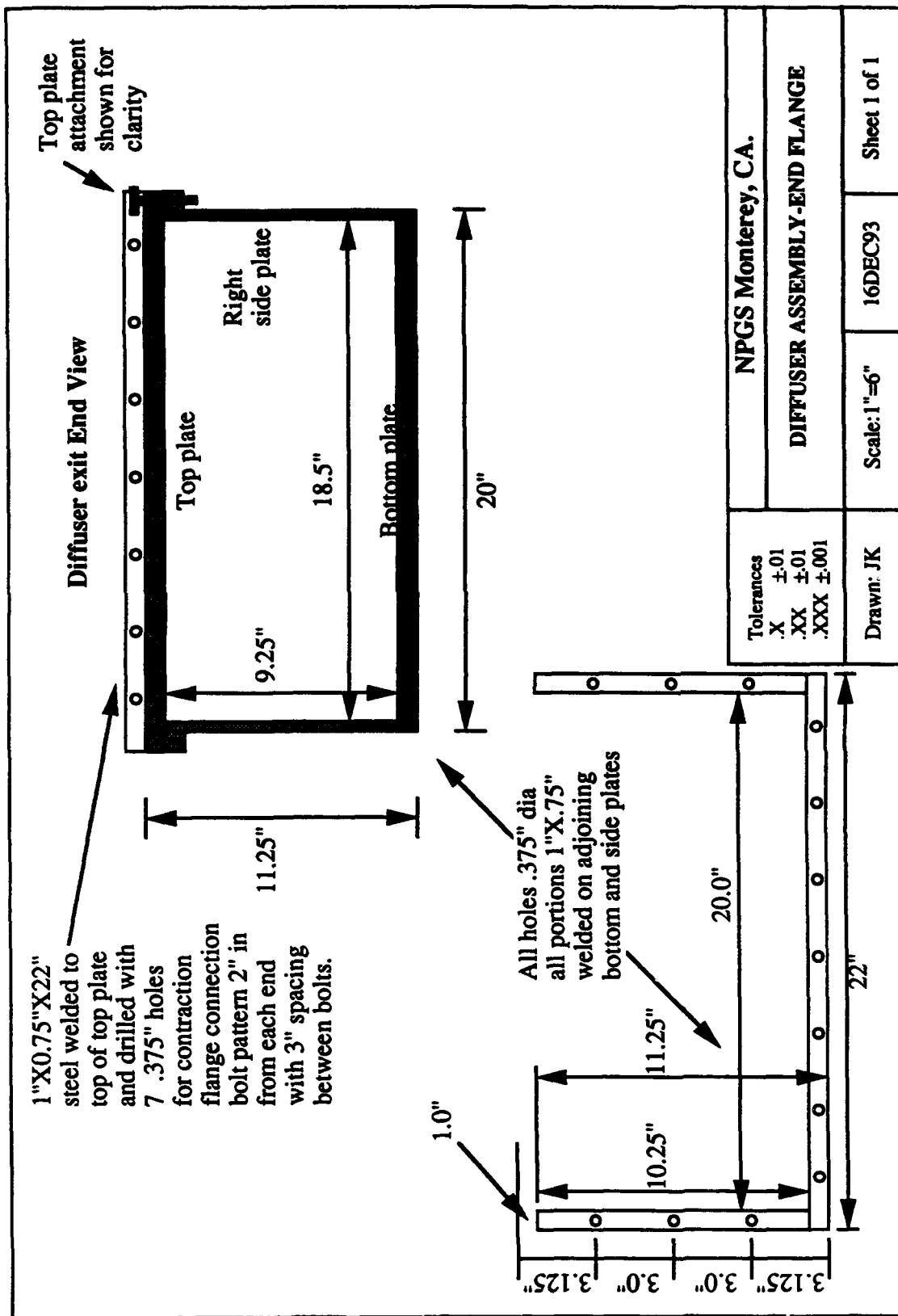
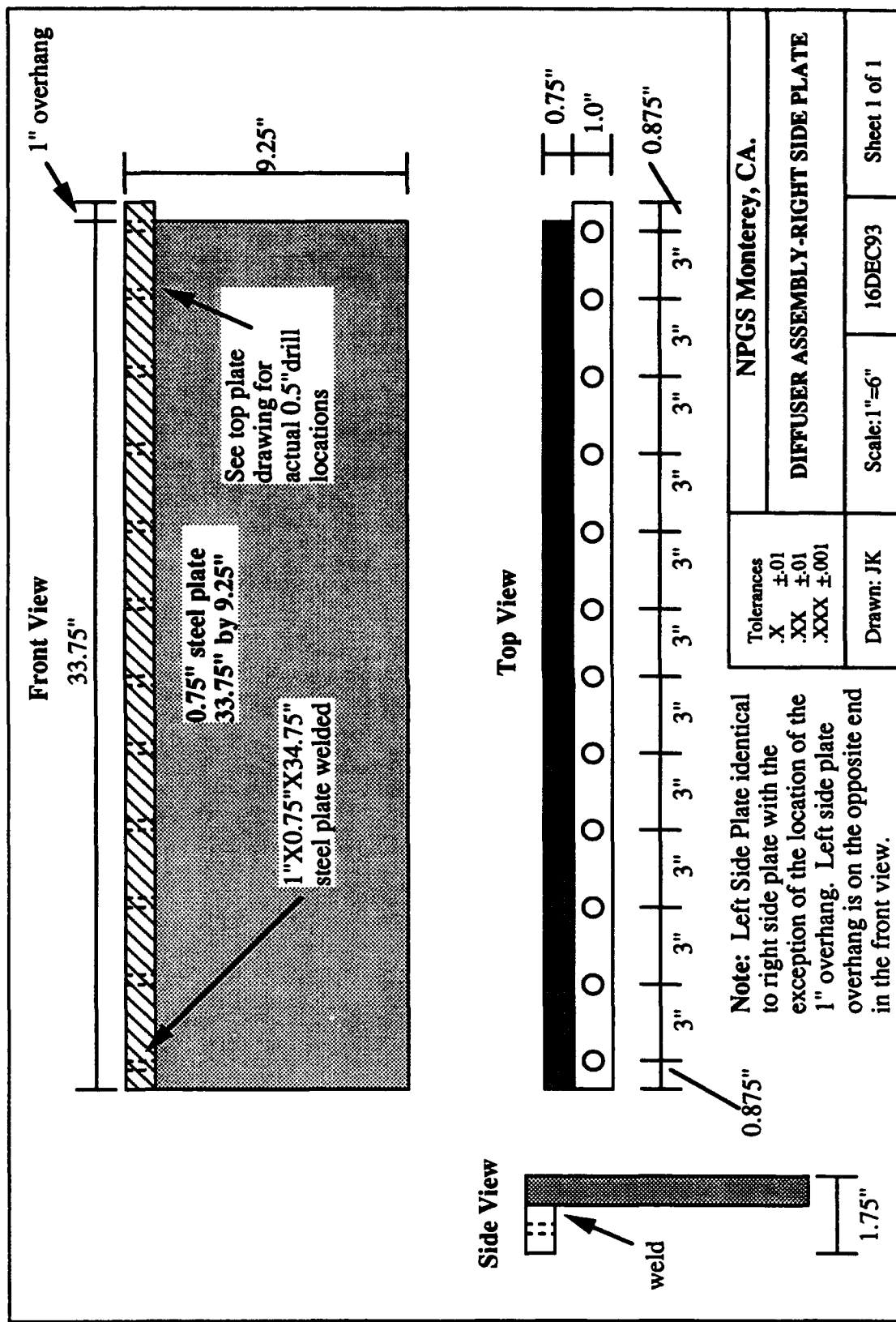


Figure 3.7 Diffuser Assembly End Flange



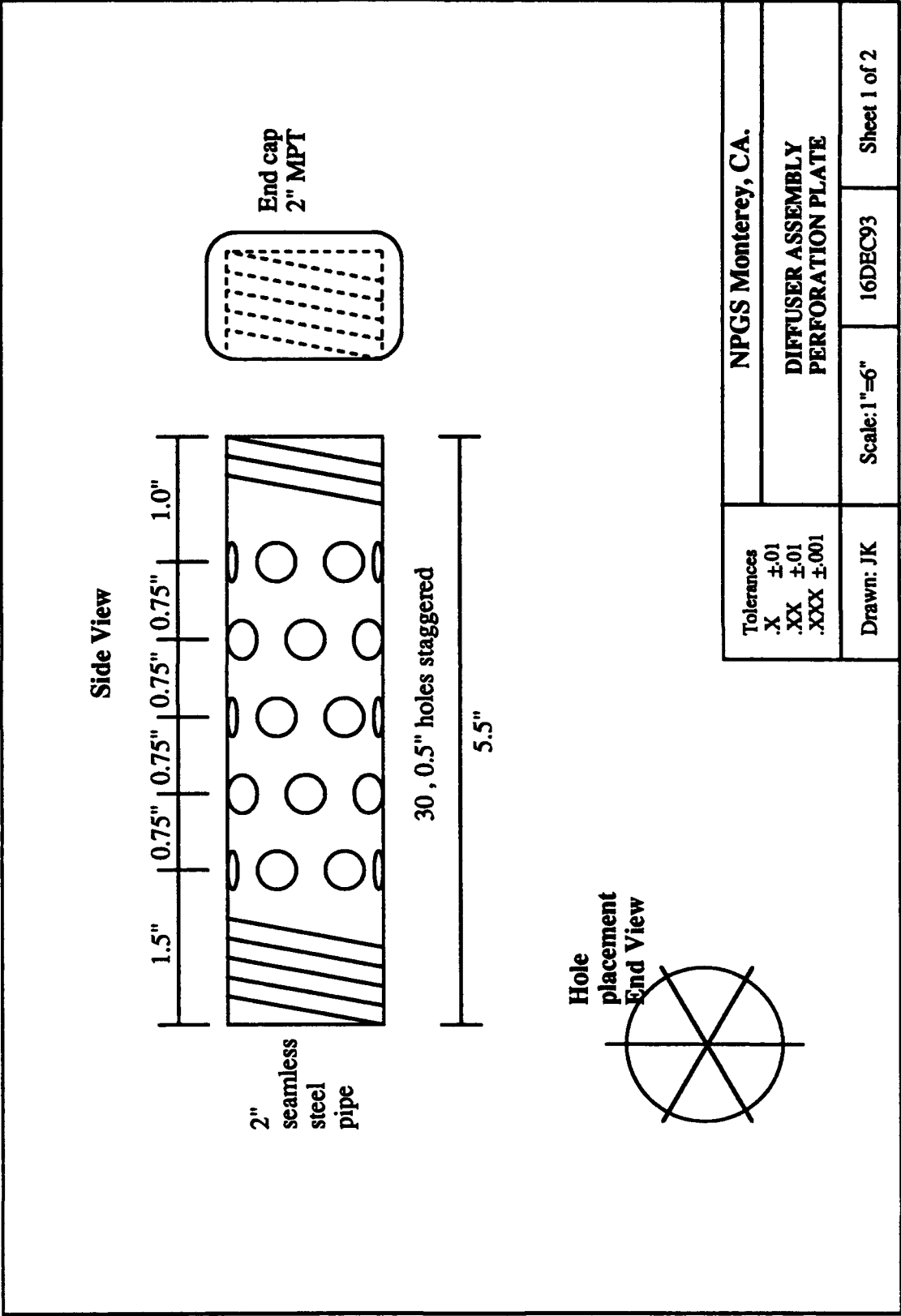


Figure 3.9 Diffuser Assembly Perforation Plates

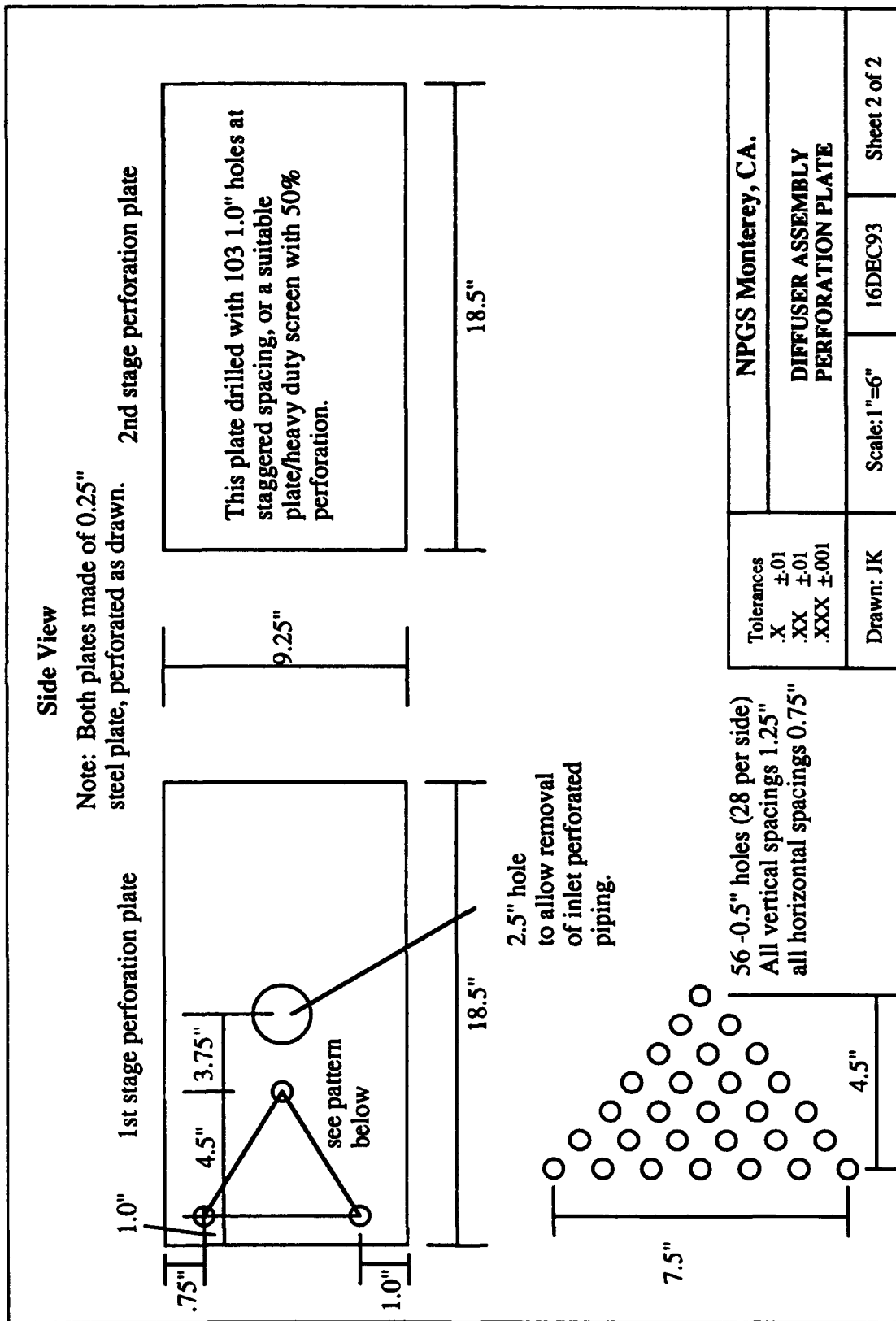


Figure 3.10 Diffuser Assembly Perforation Plates

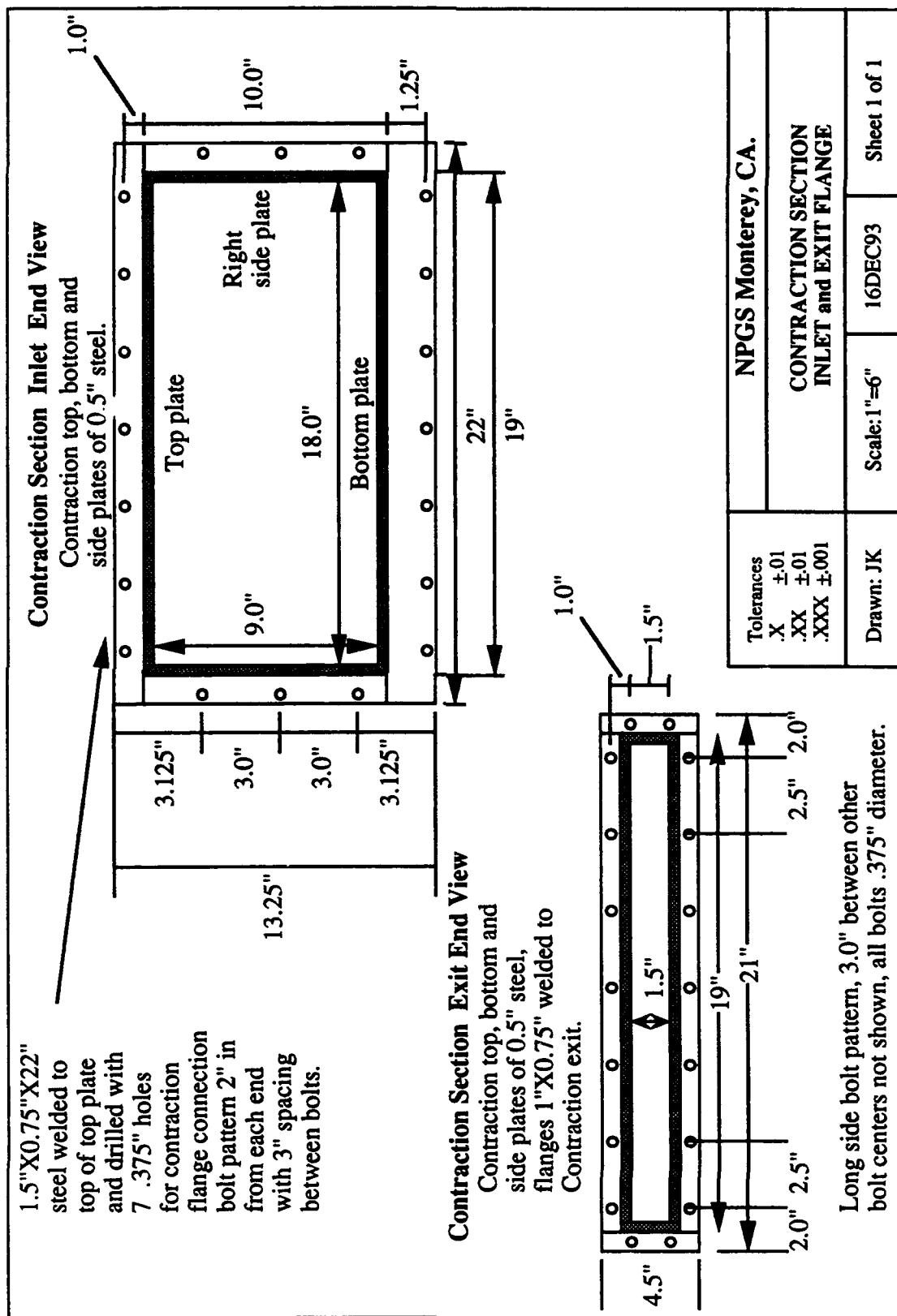


Figure 3.11 Contraction Section Inlet and Exit Flange

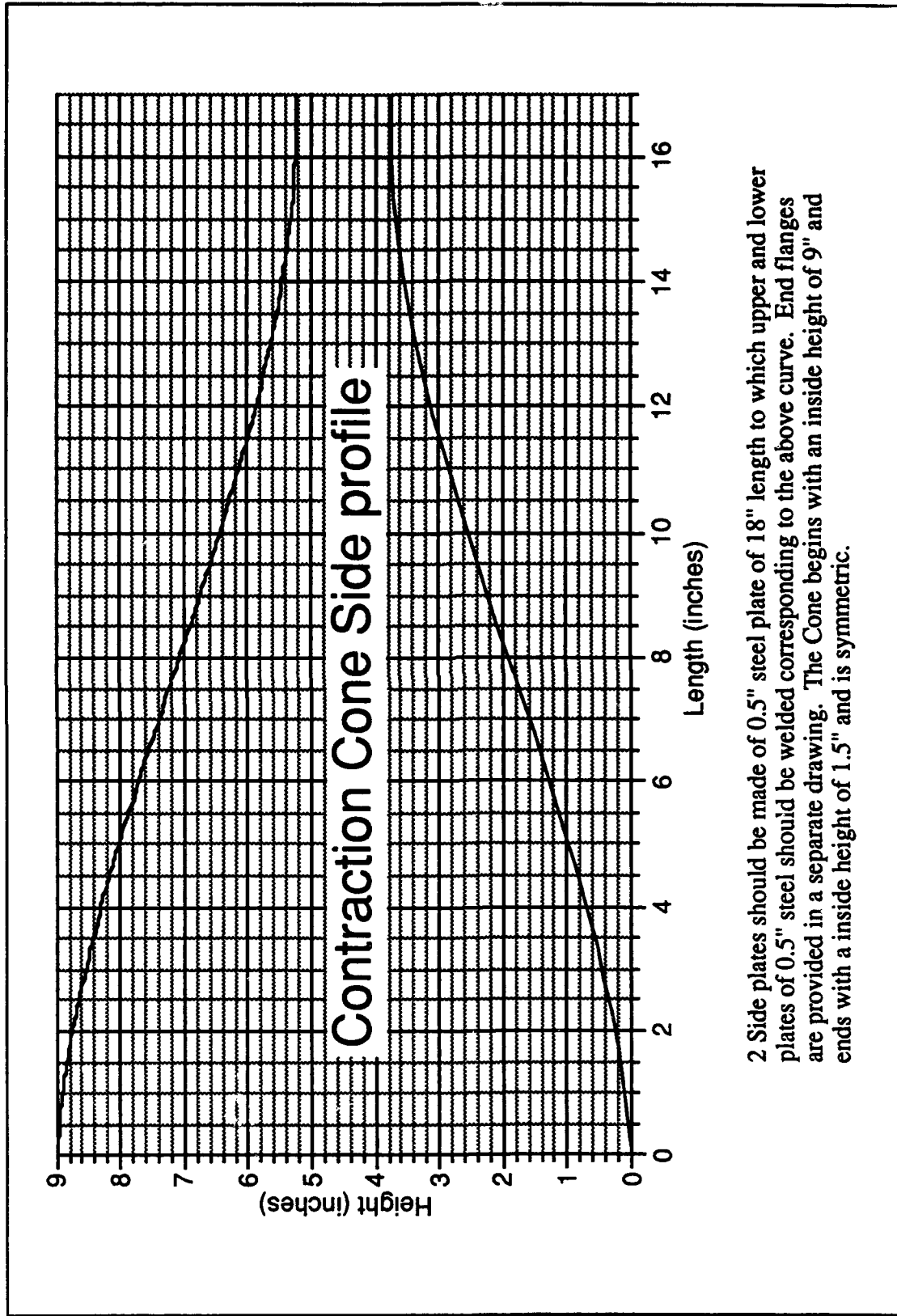


Figure 3.12 Contraction Cone Side Plate

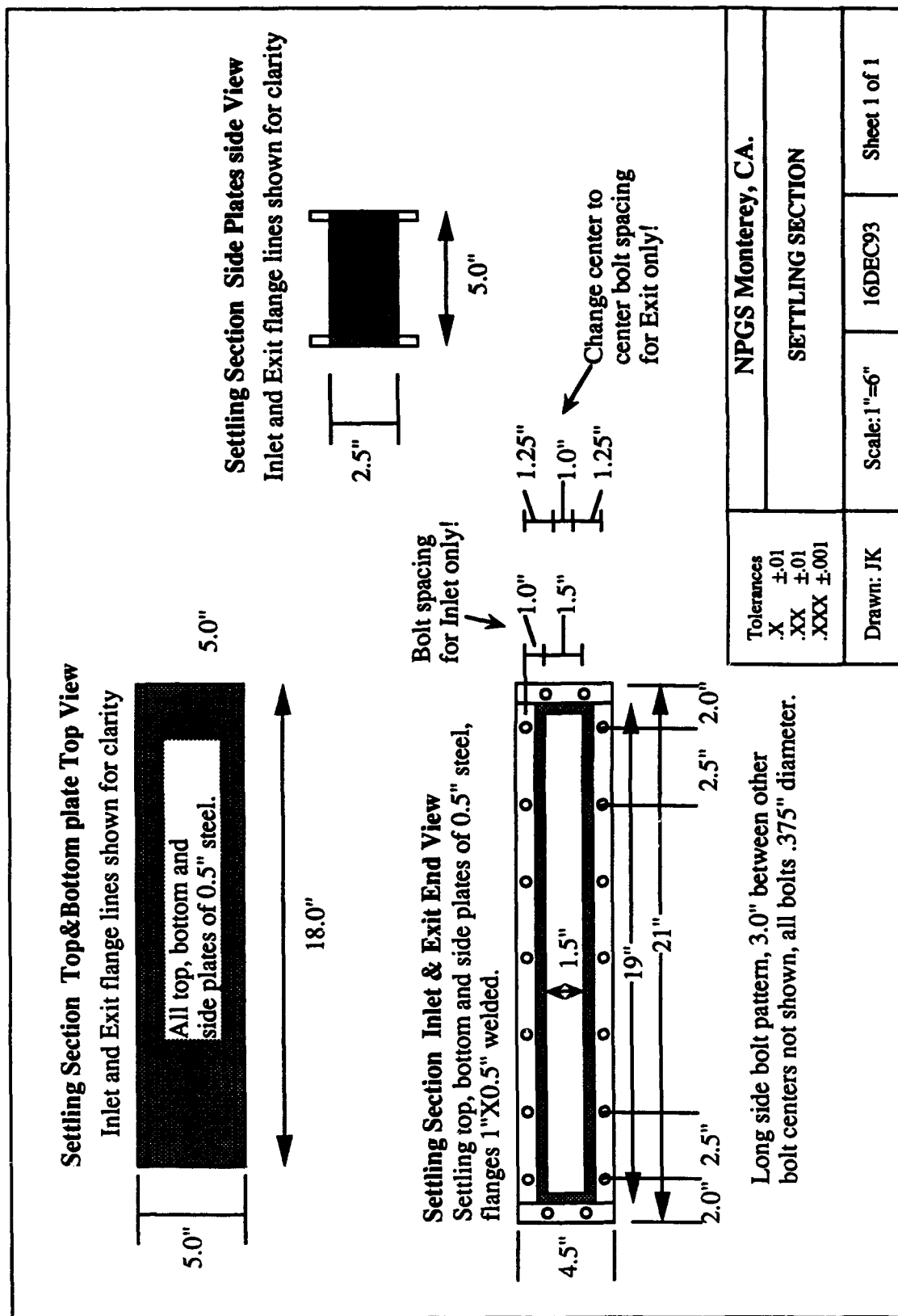


Figure 3.13 Settling Section

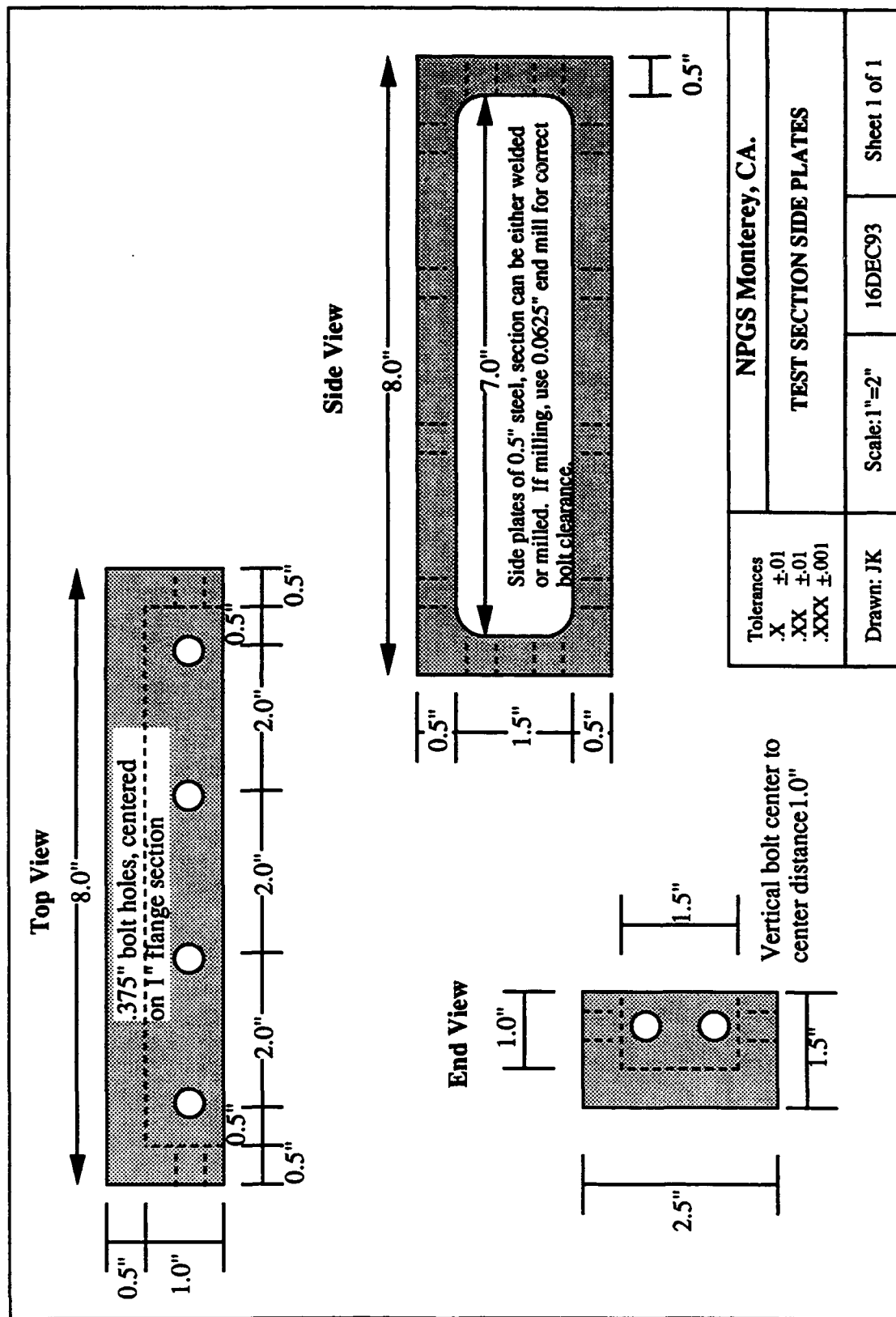


Figure 3.14 Test Section Side Plates

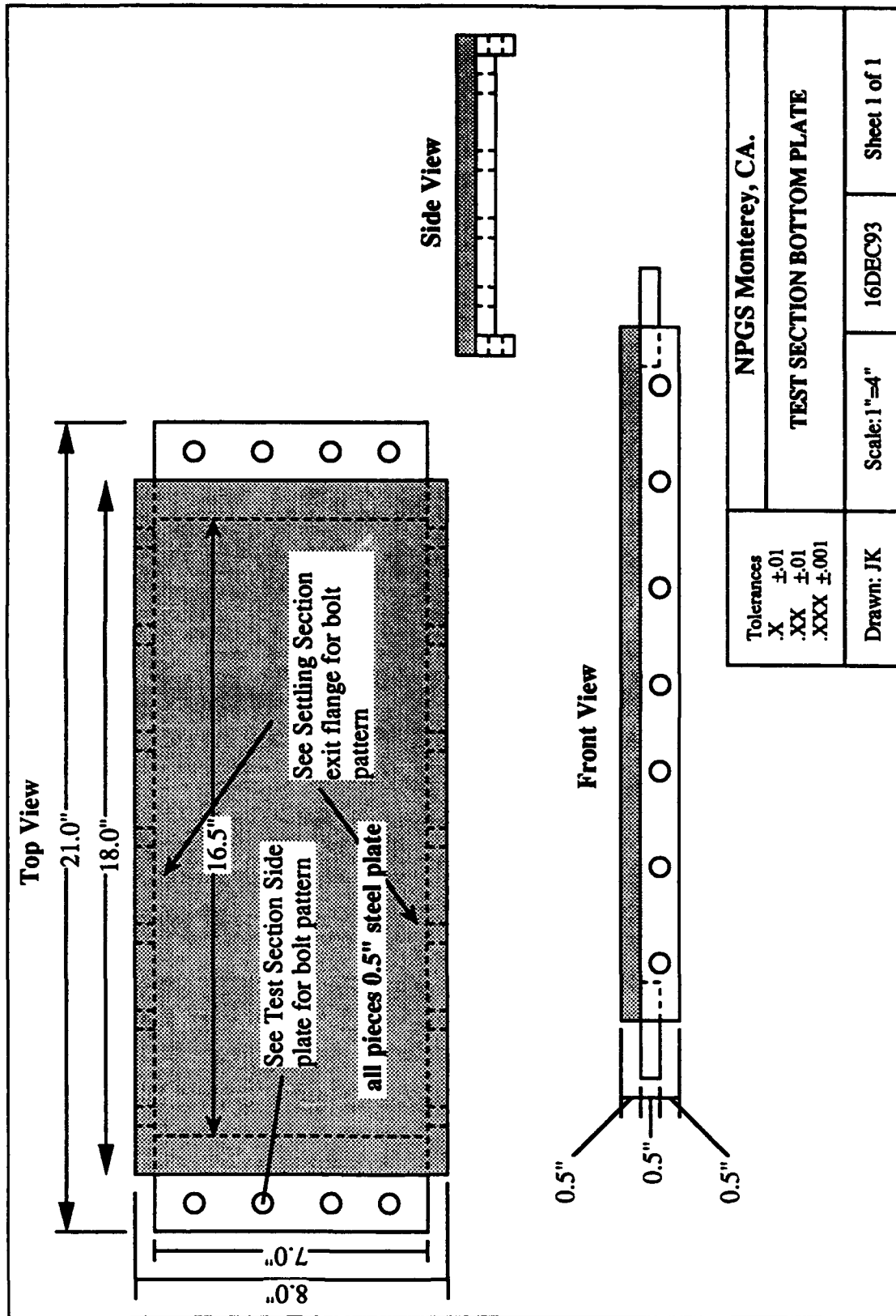


Figure 3.15 Test Section Bottom Plate

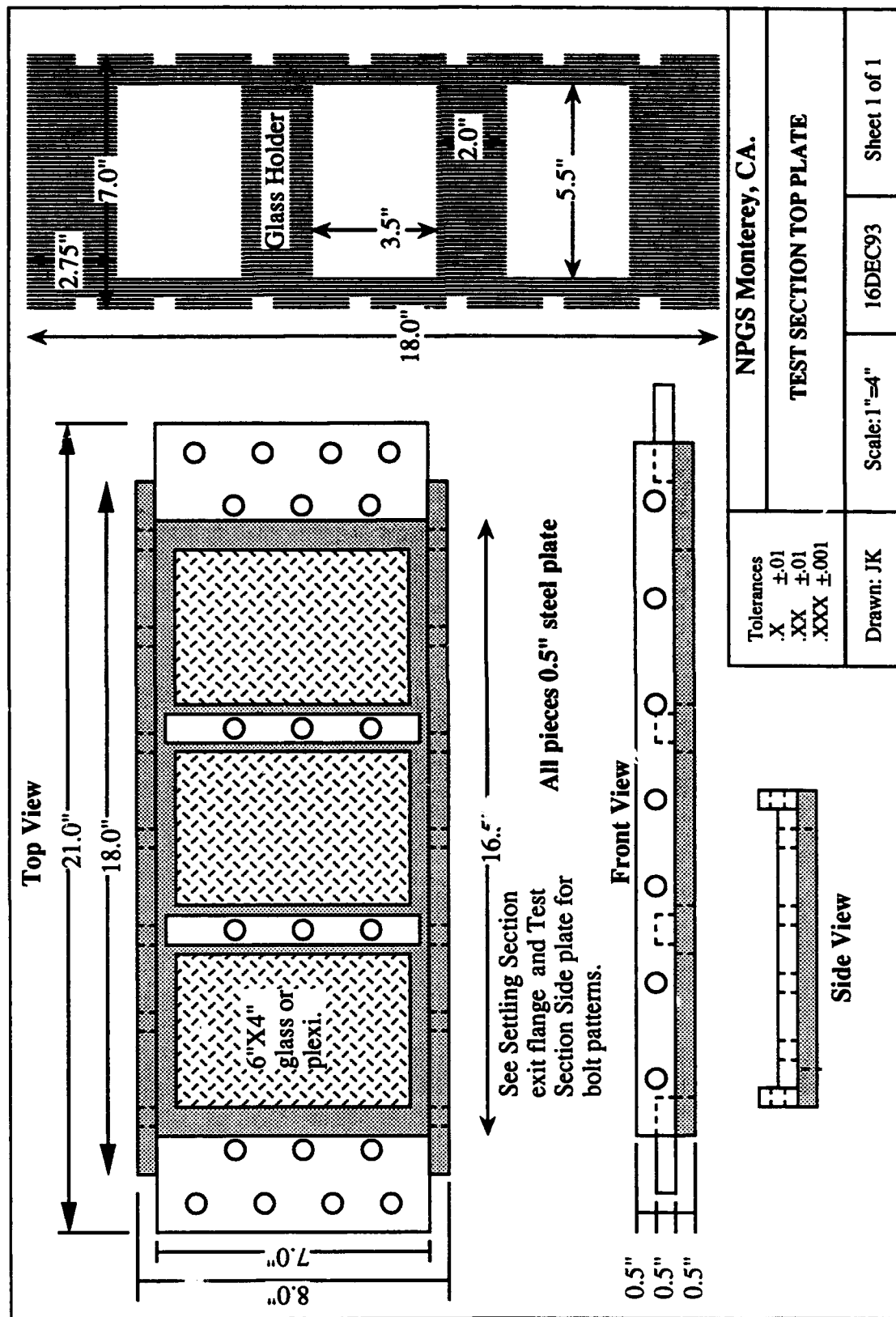


Figure 3.16 Test Section Top Plate

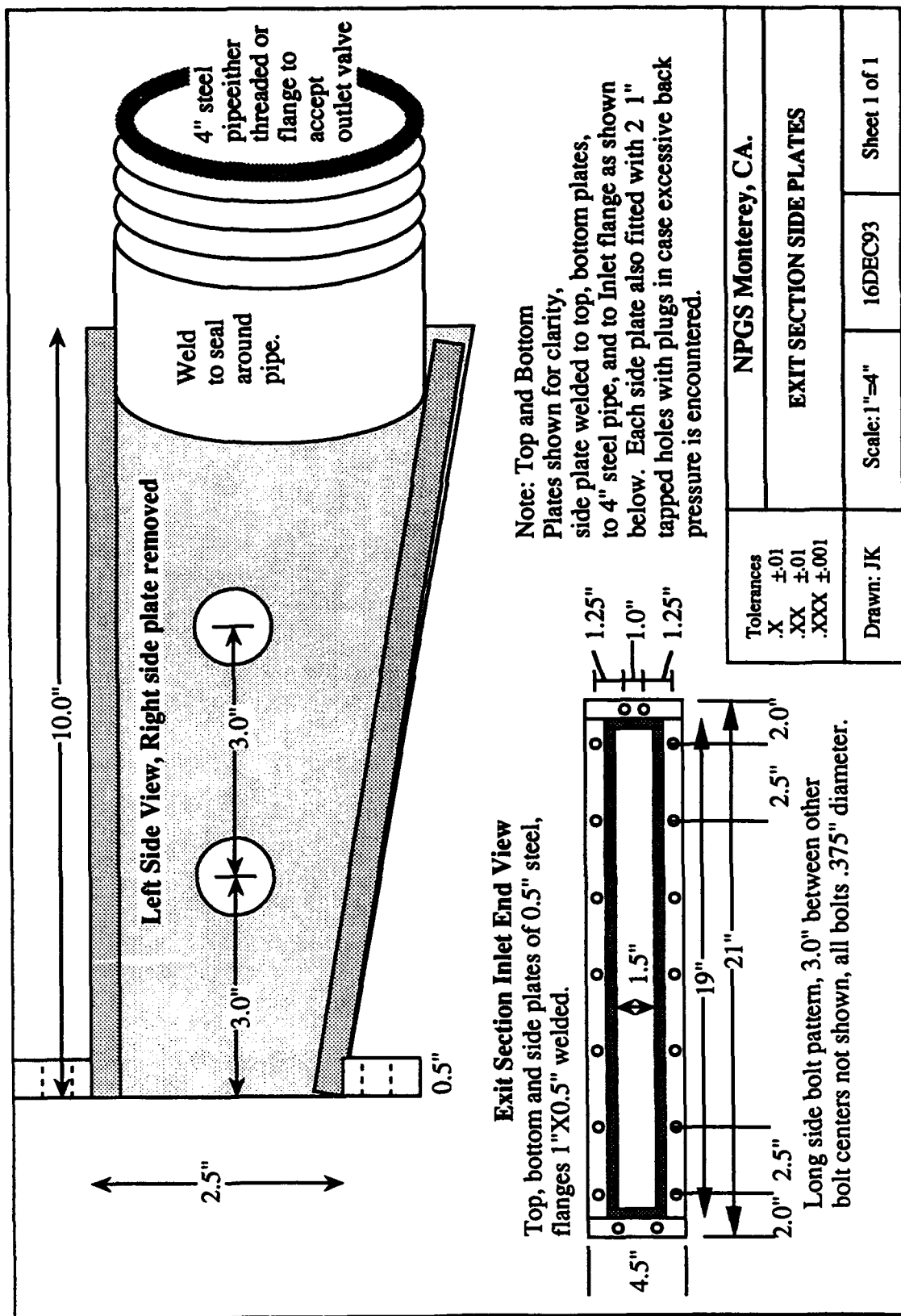


Figure 3.17 Exit Section Side Plates

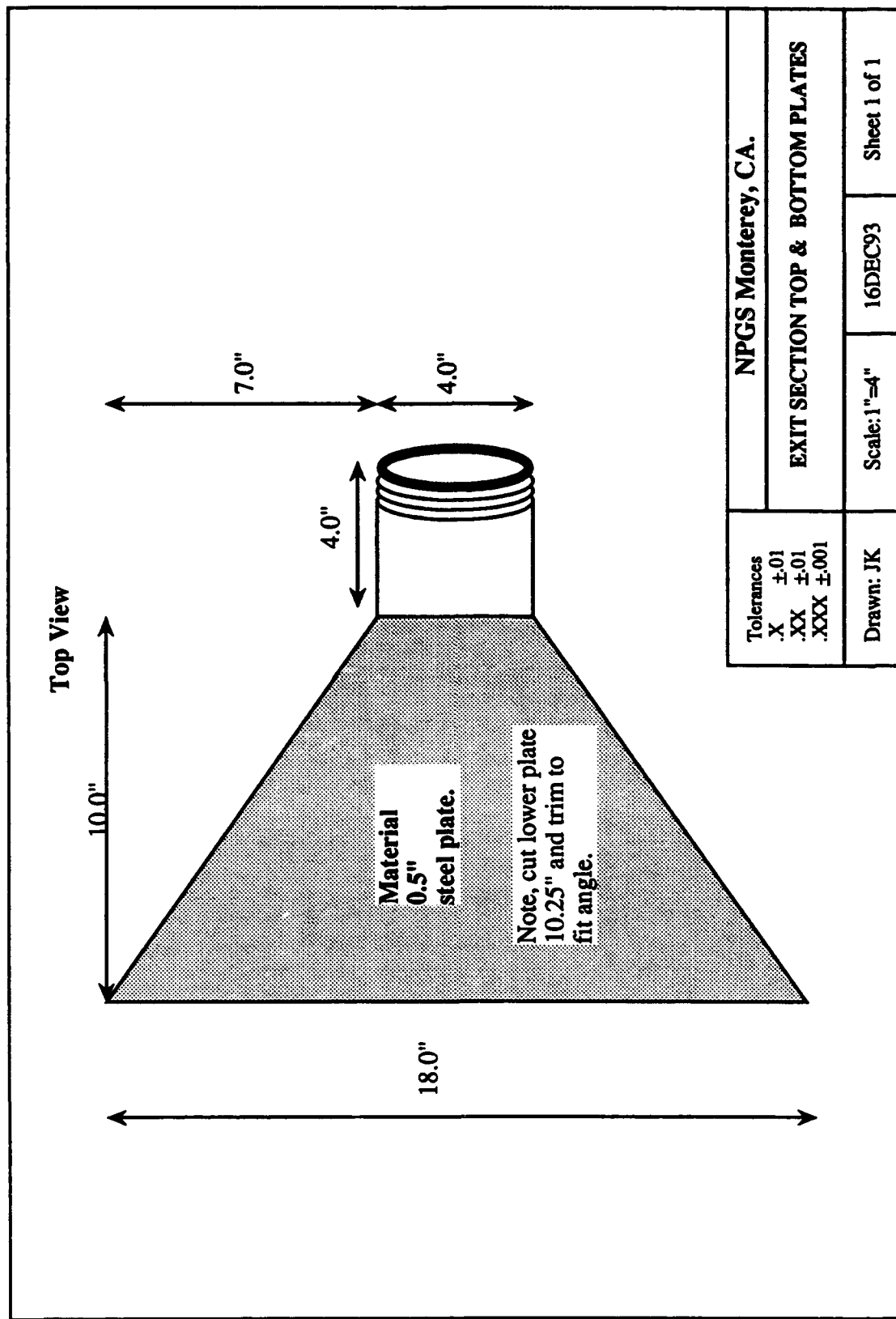


Figure 3.18 Exit Section Top & Bottom Plates

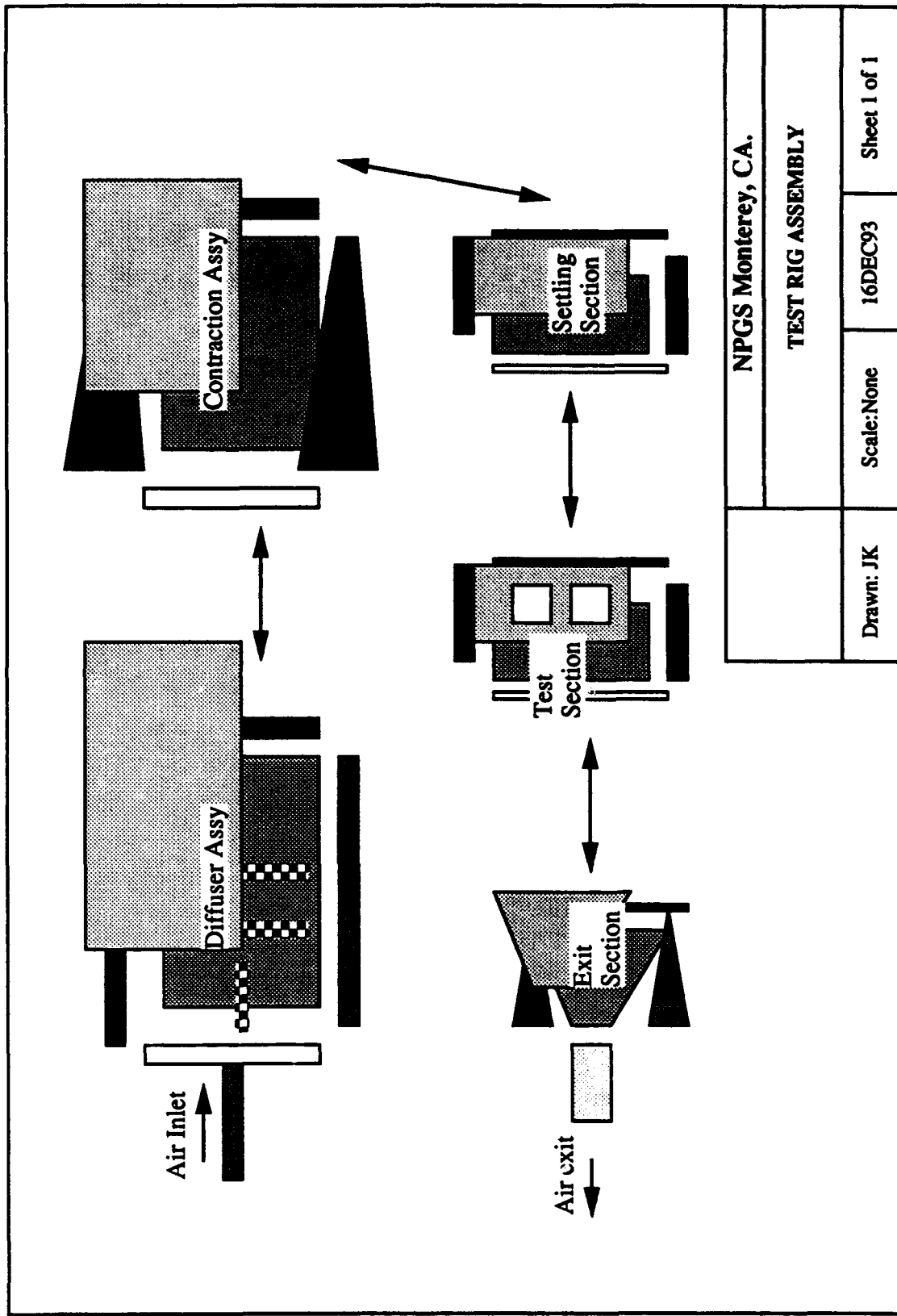


Figure 3.19 Test Rig Assembly

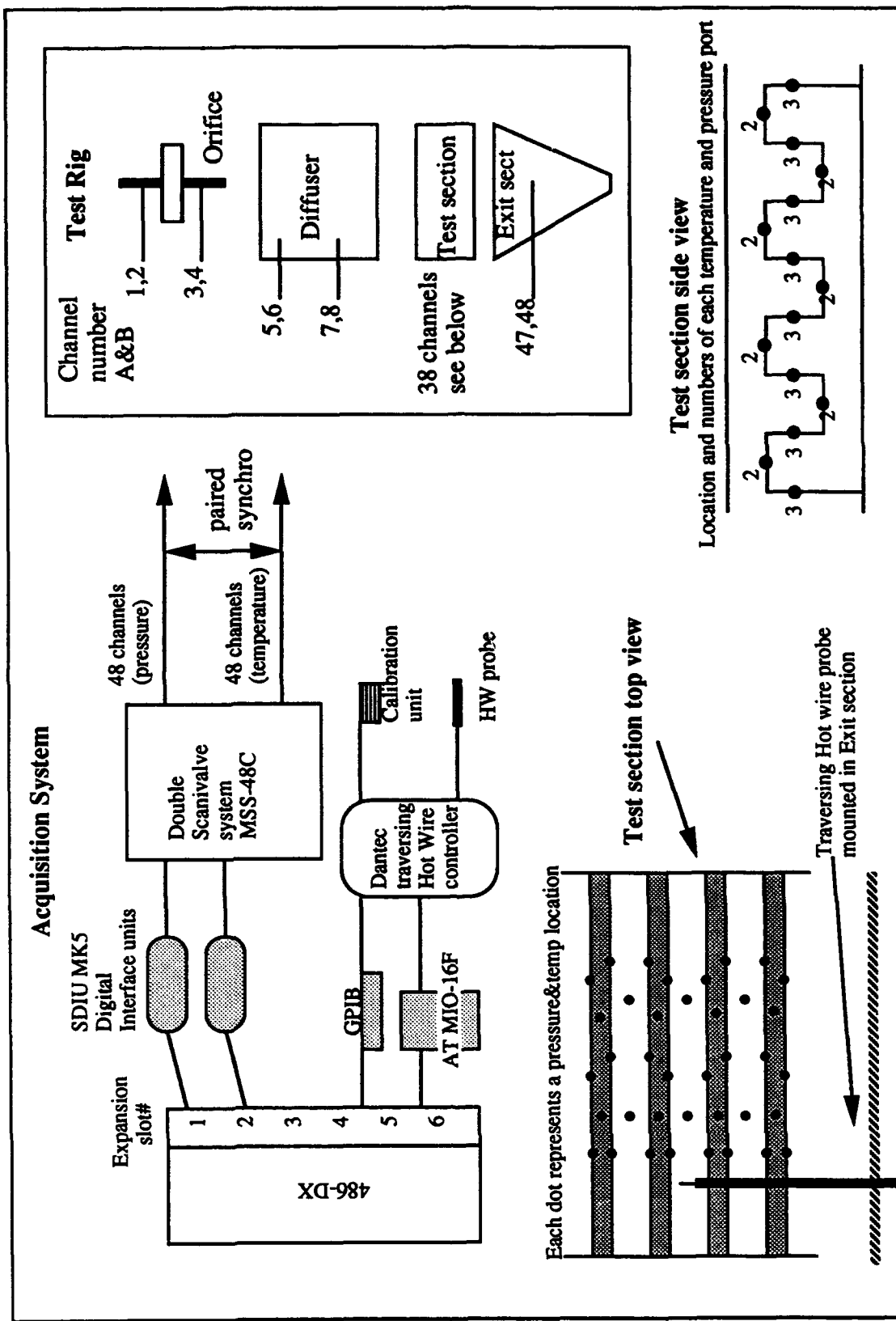


Figure 4.1 Data Acquisition Schematic

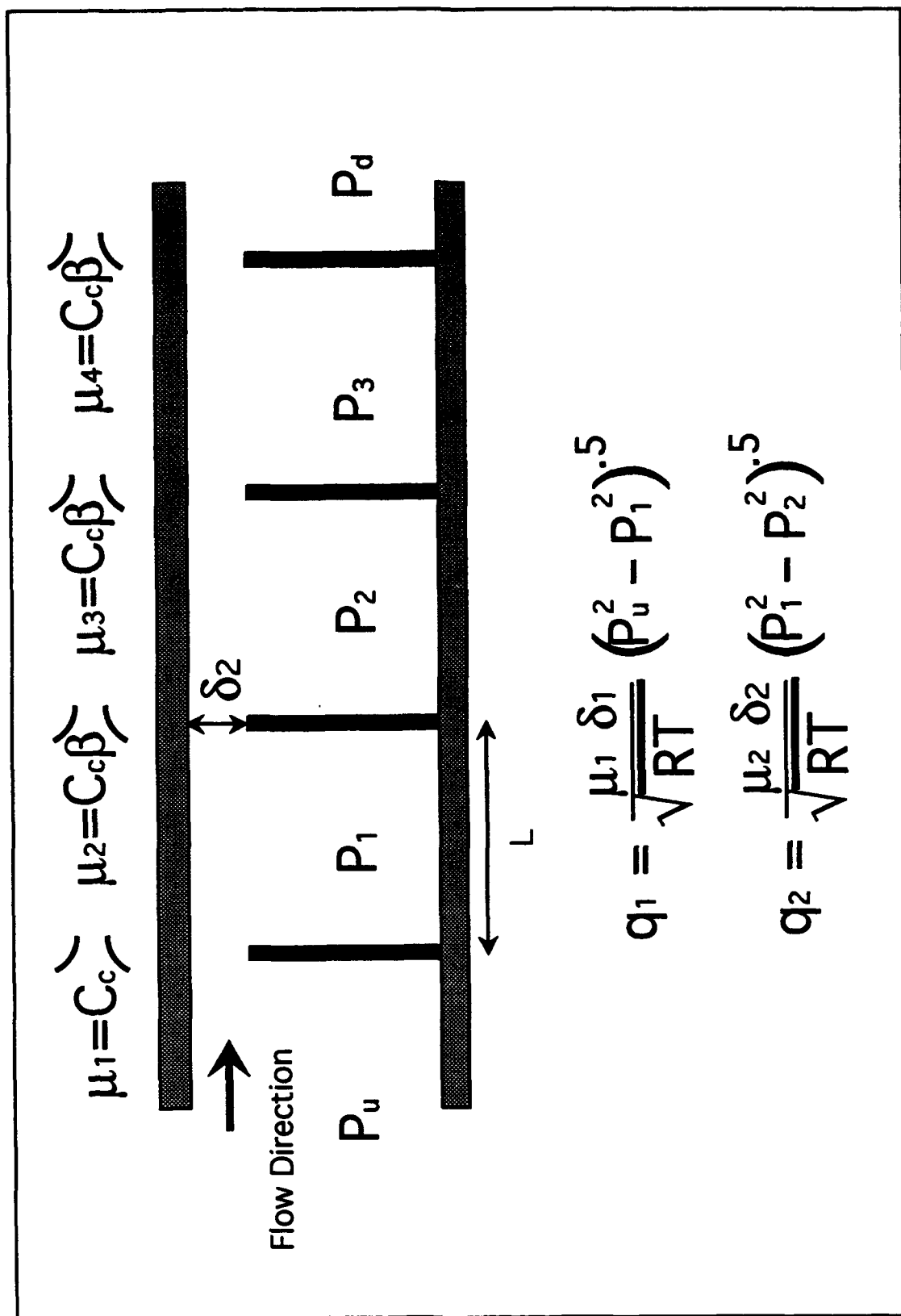


Figure 5.1 Labyrinth Seal Diagram

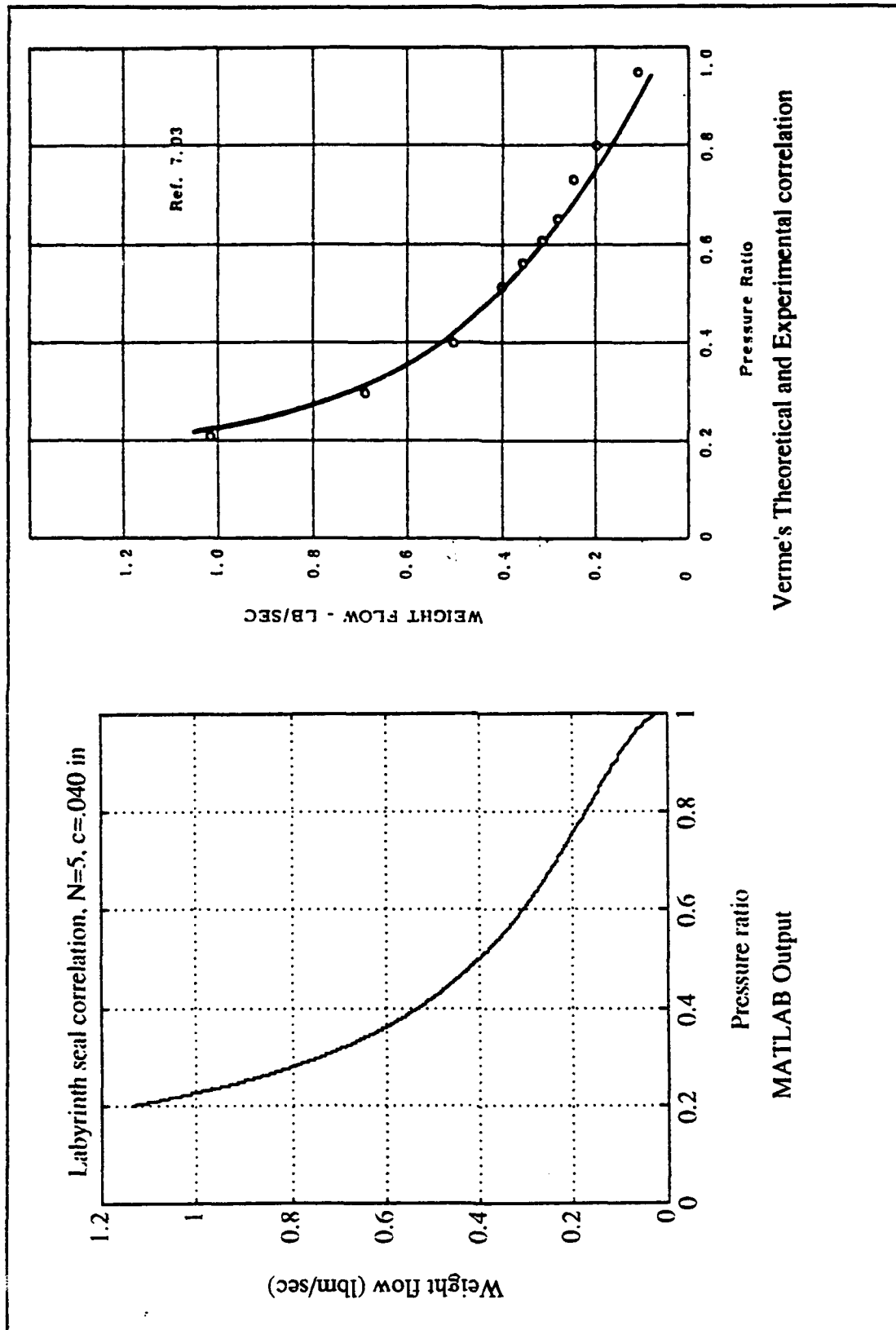


Figure 5.2 Flow Rate Correlation

MATLAB Output

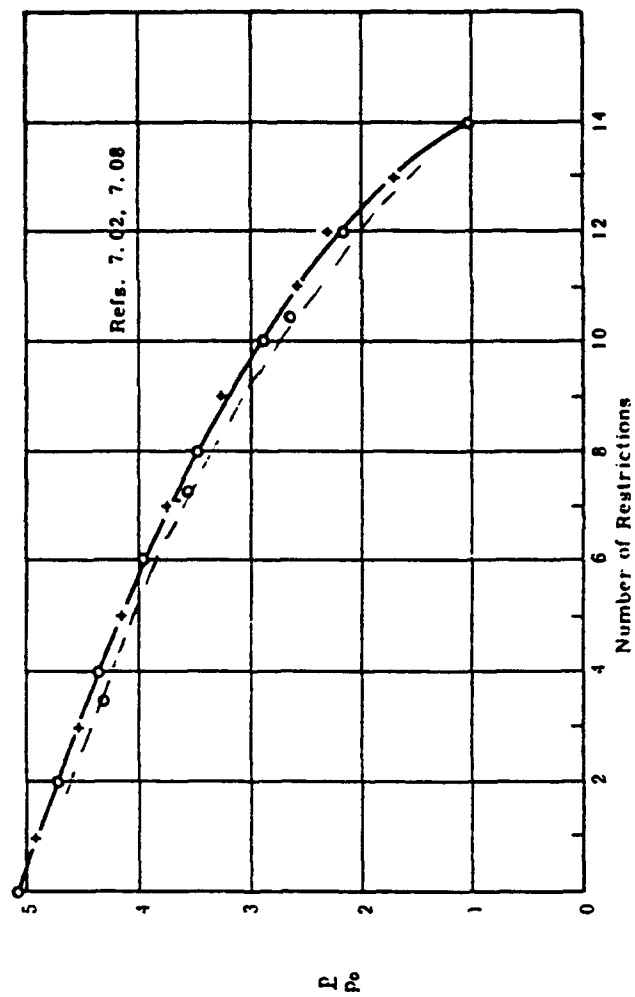


Fig. 7-11 Distribution of Chamber Pressures along Labyrinth for $p_0/p_N = 5$

Figure 5.3 Chamber Pressure Correlation

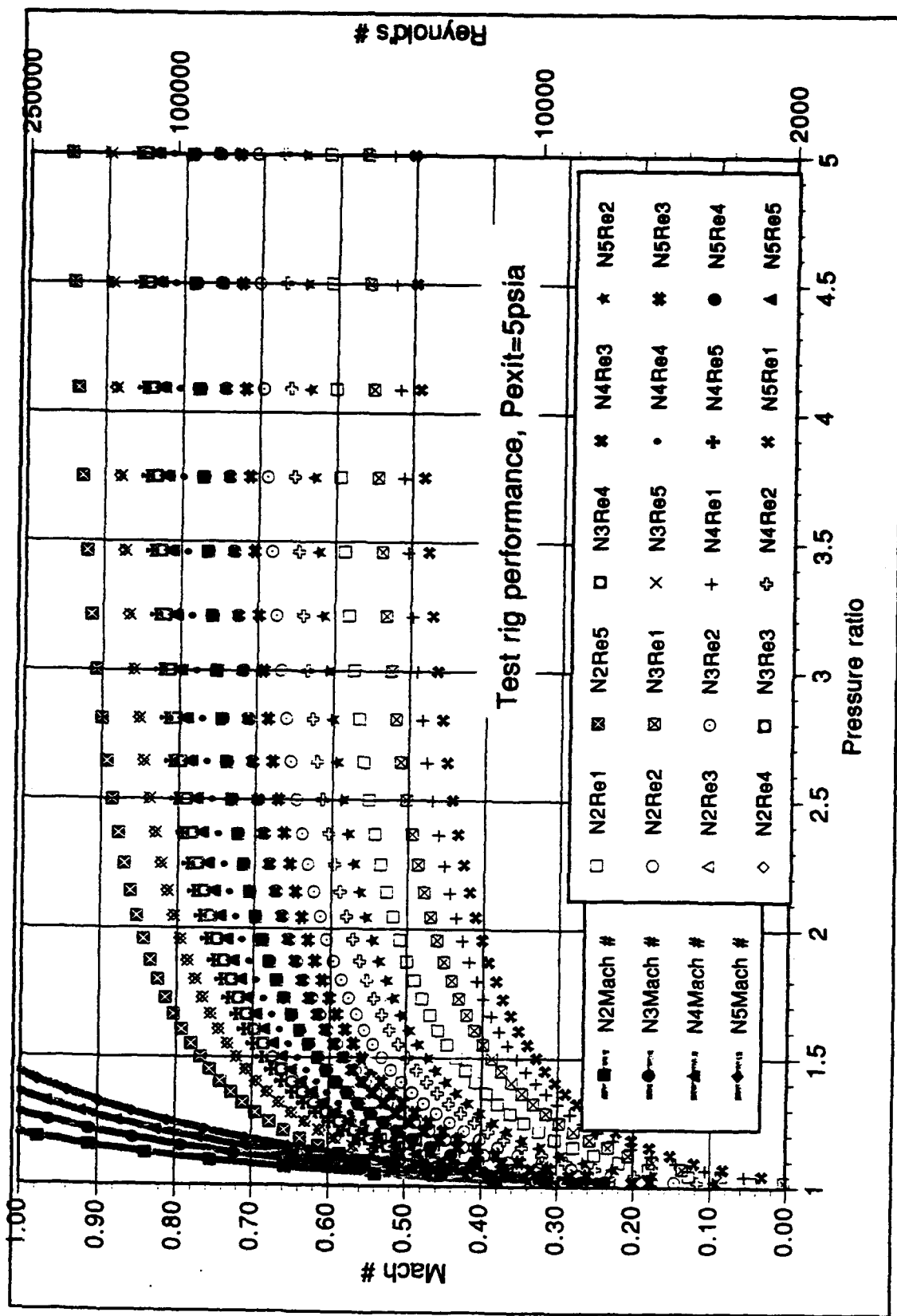


Figure 5.4 Test Rig Performance

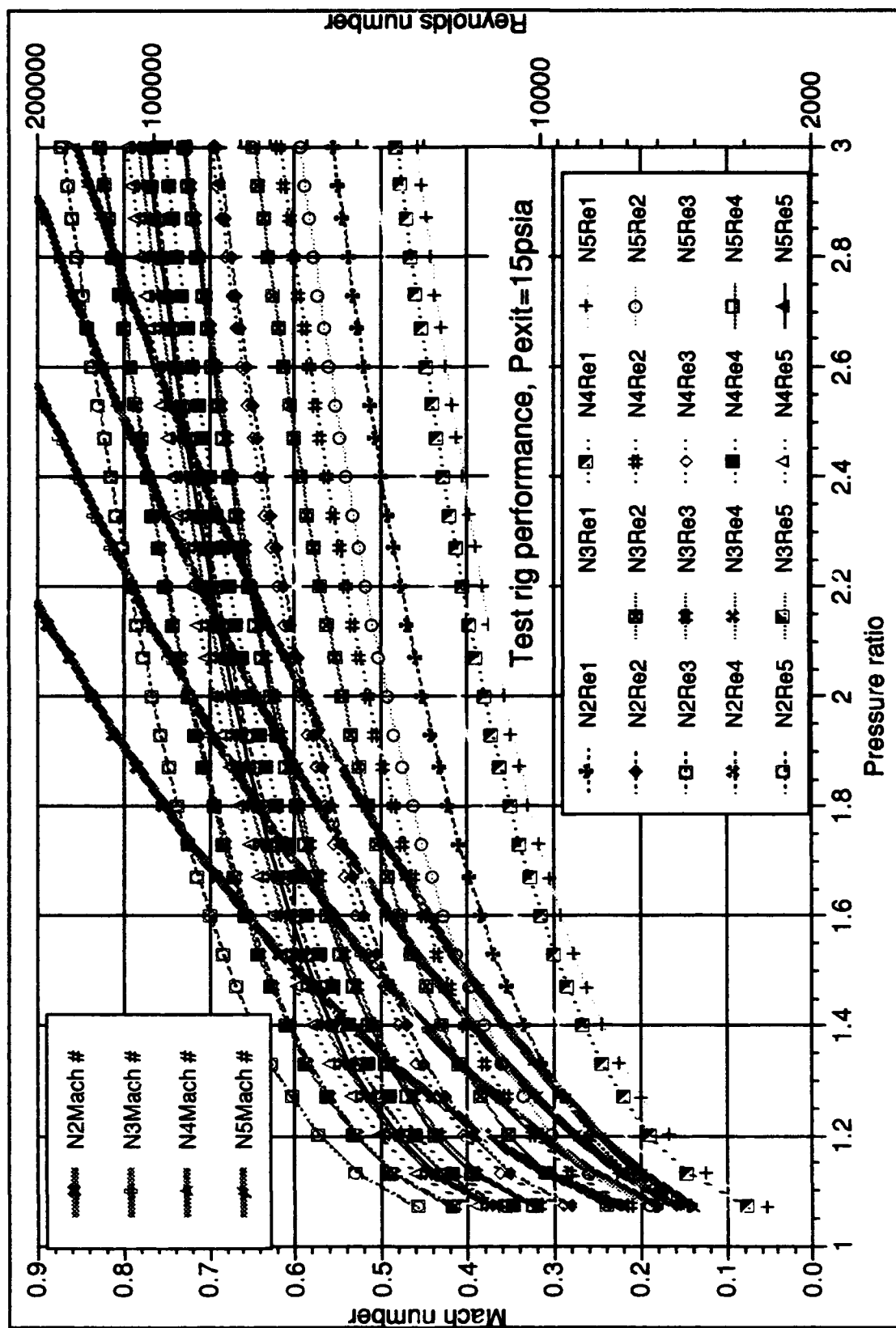


Figure 5.5 Test Rig Performance

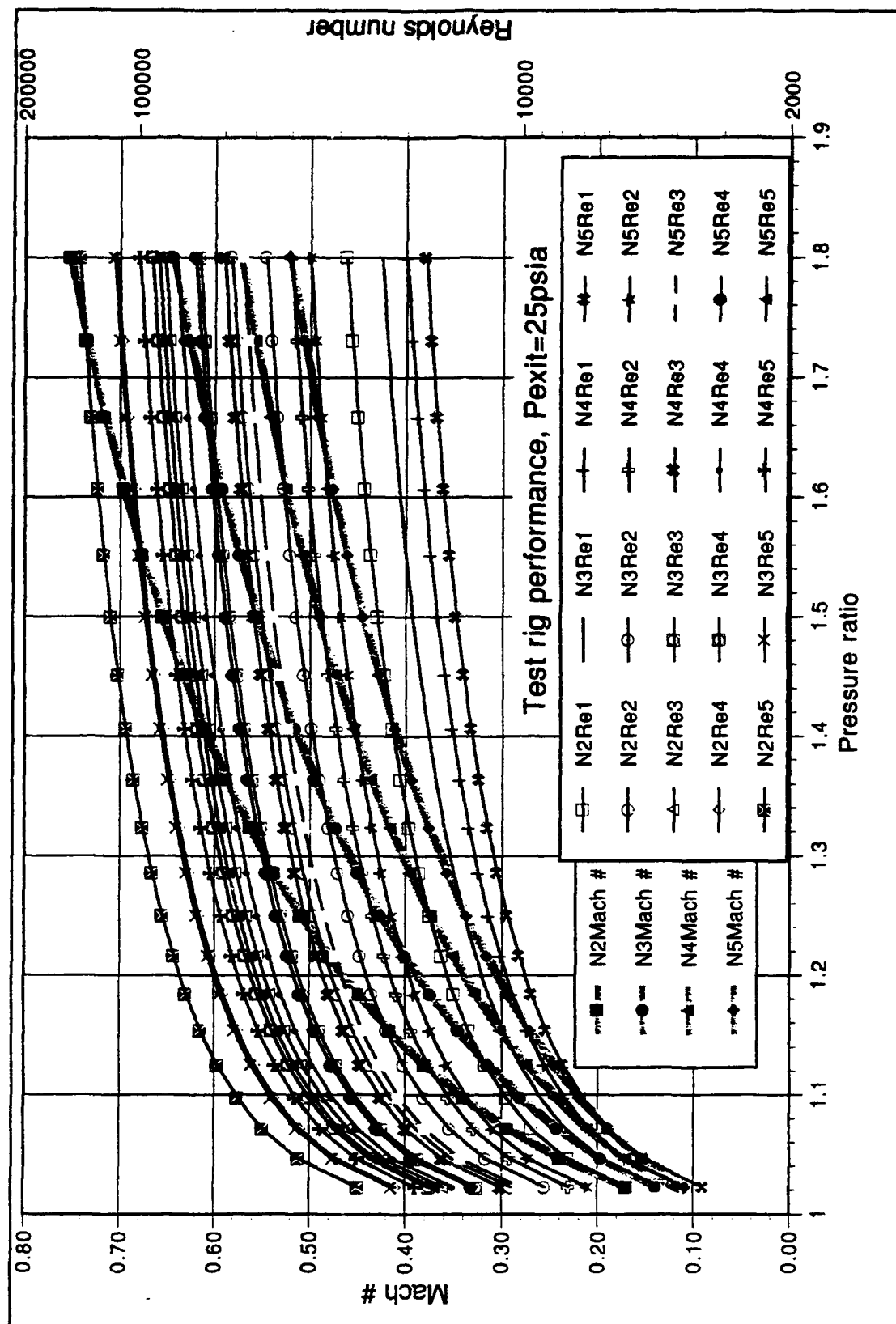


Figure 5.6 Test Rig Performance

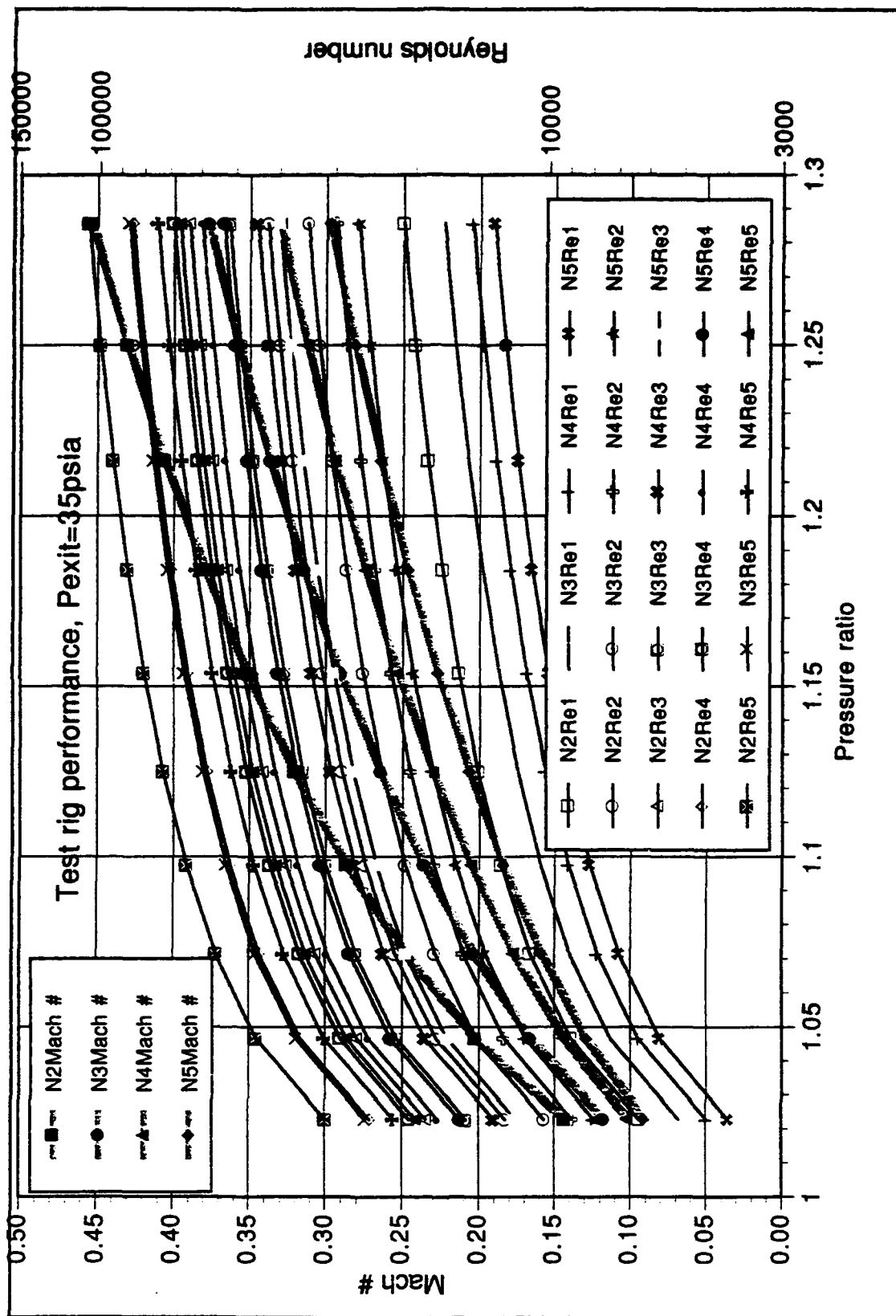


Figure 5.7 Test Rig Performance

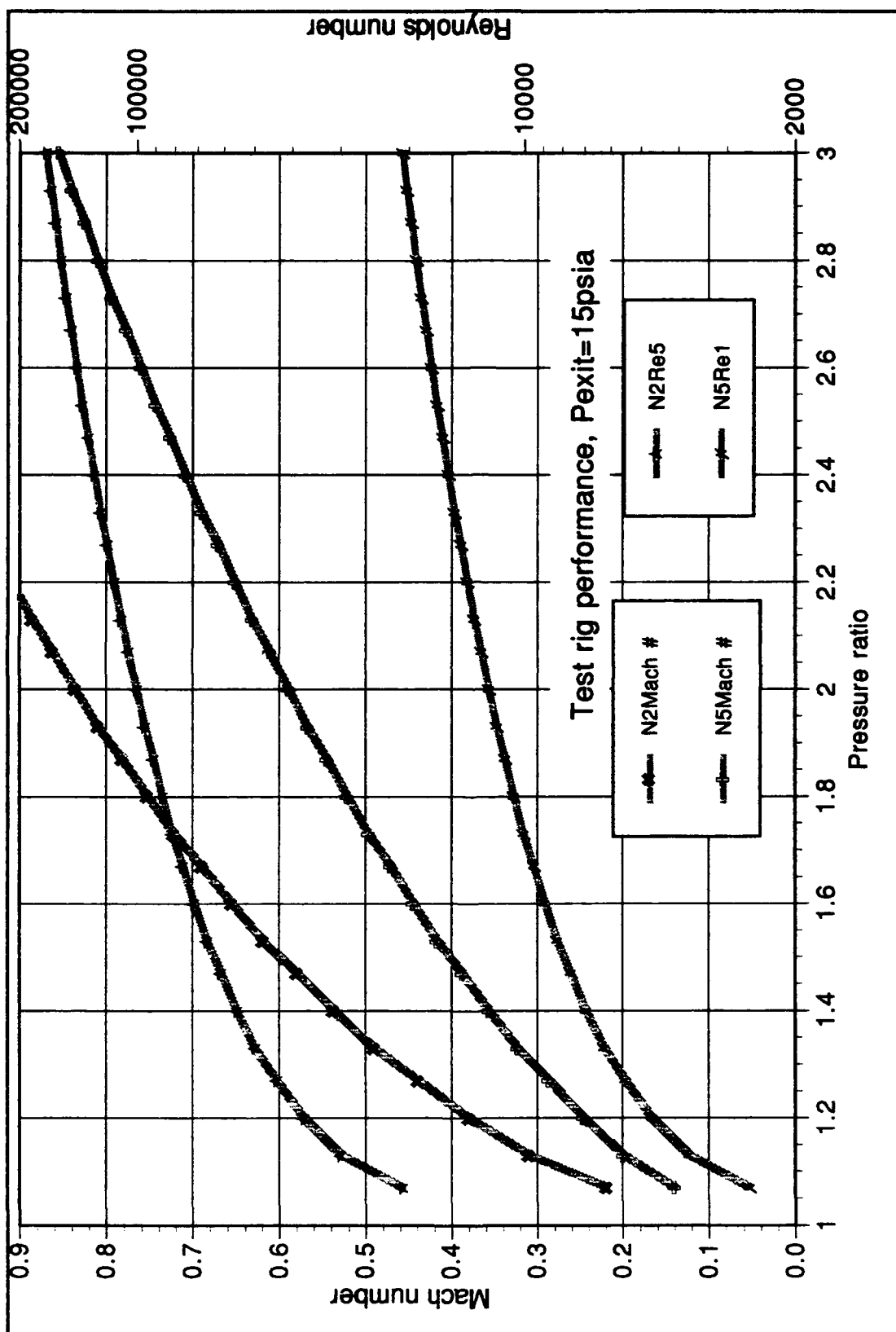


Figure 5.8 Test Rig Performance

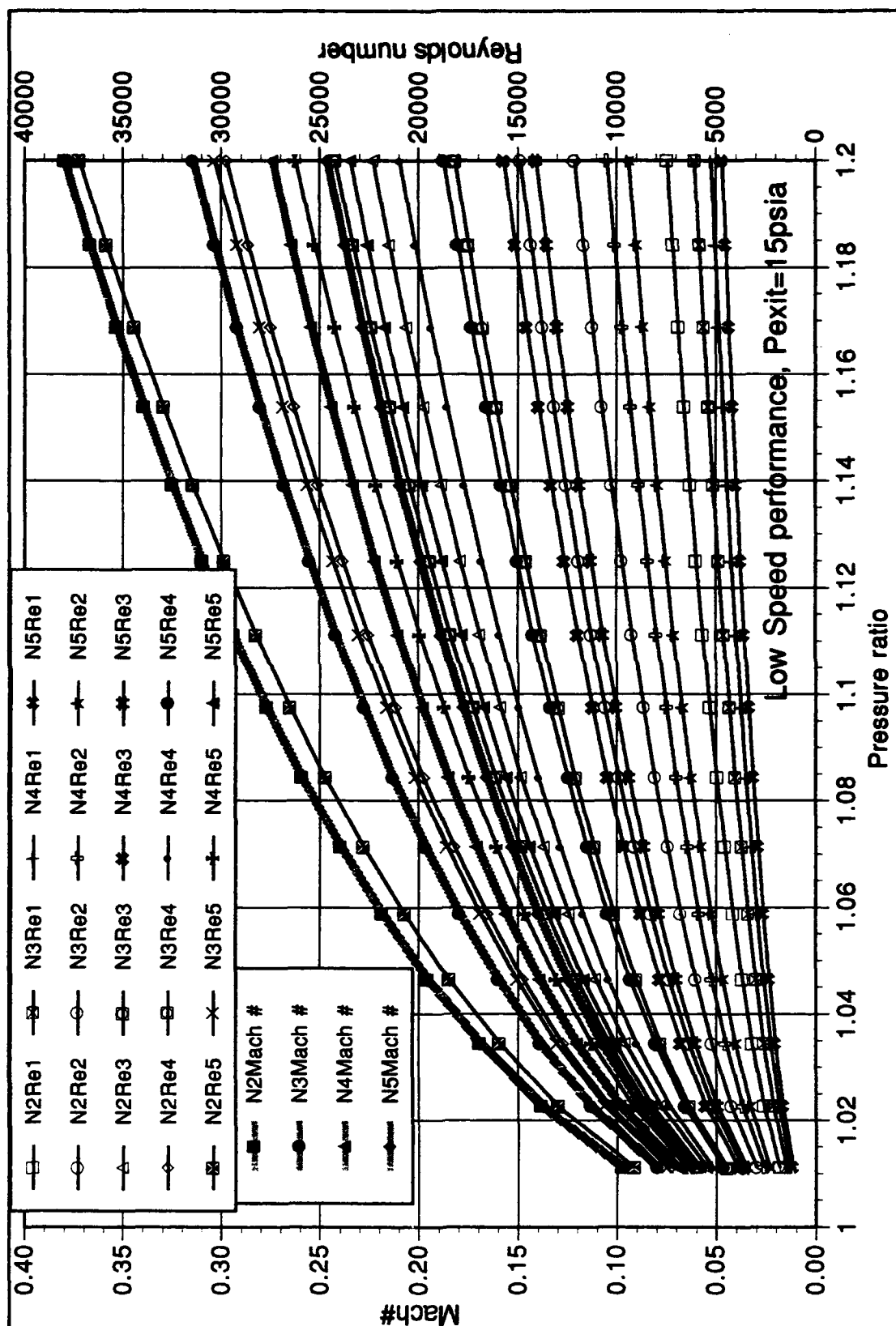


Figure 5.9 Test Rig Performance

Mach number Vs Reynolds number Back-pressure effects

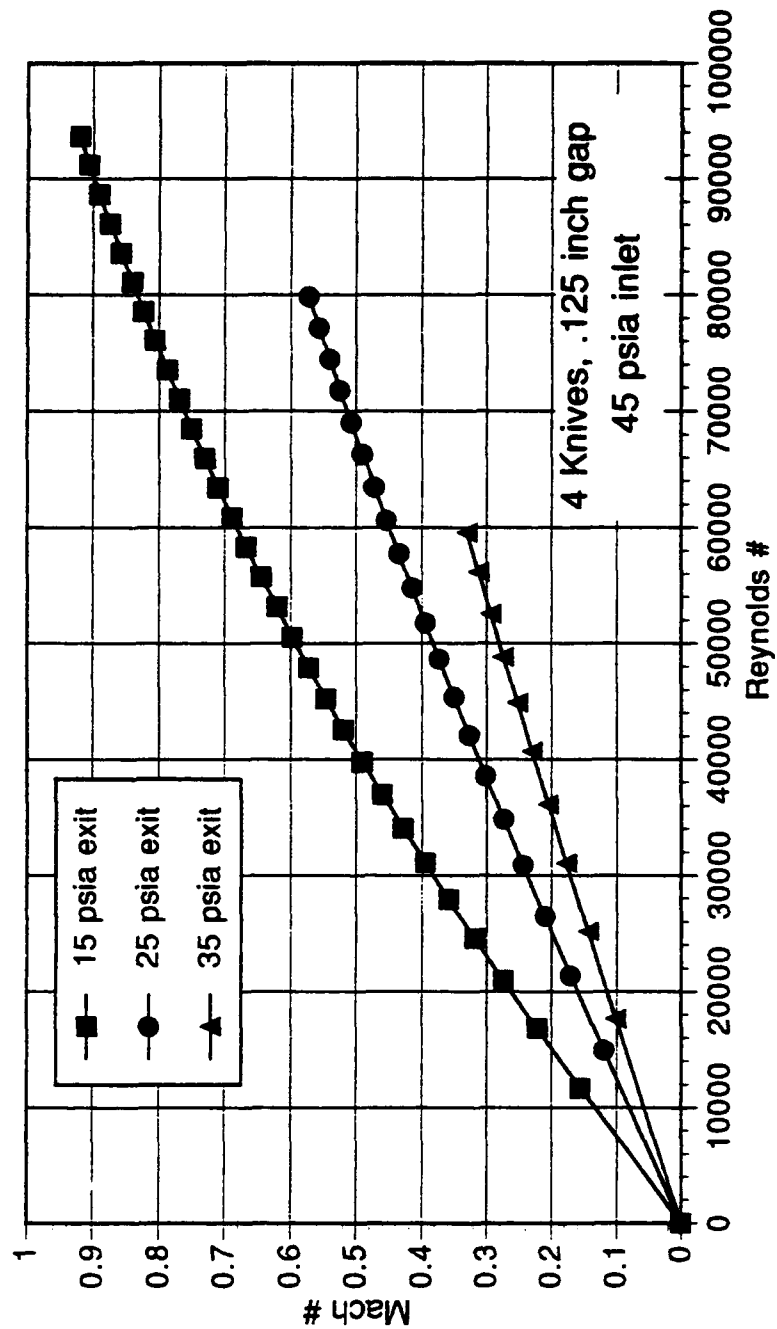


Figure 5.10 Test Rig Performance

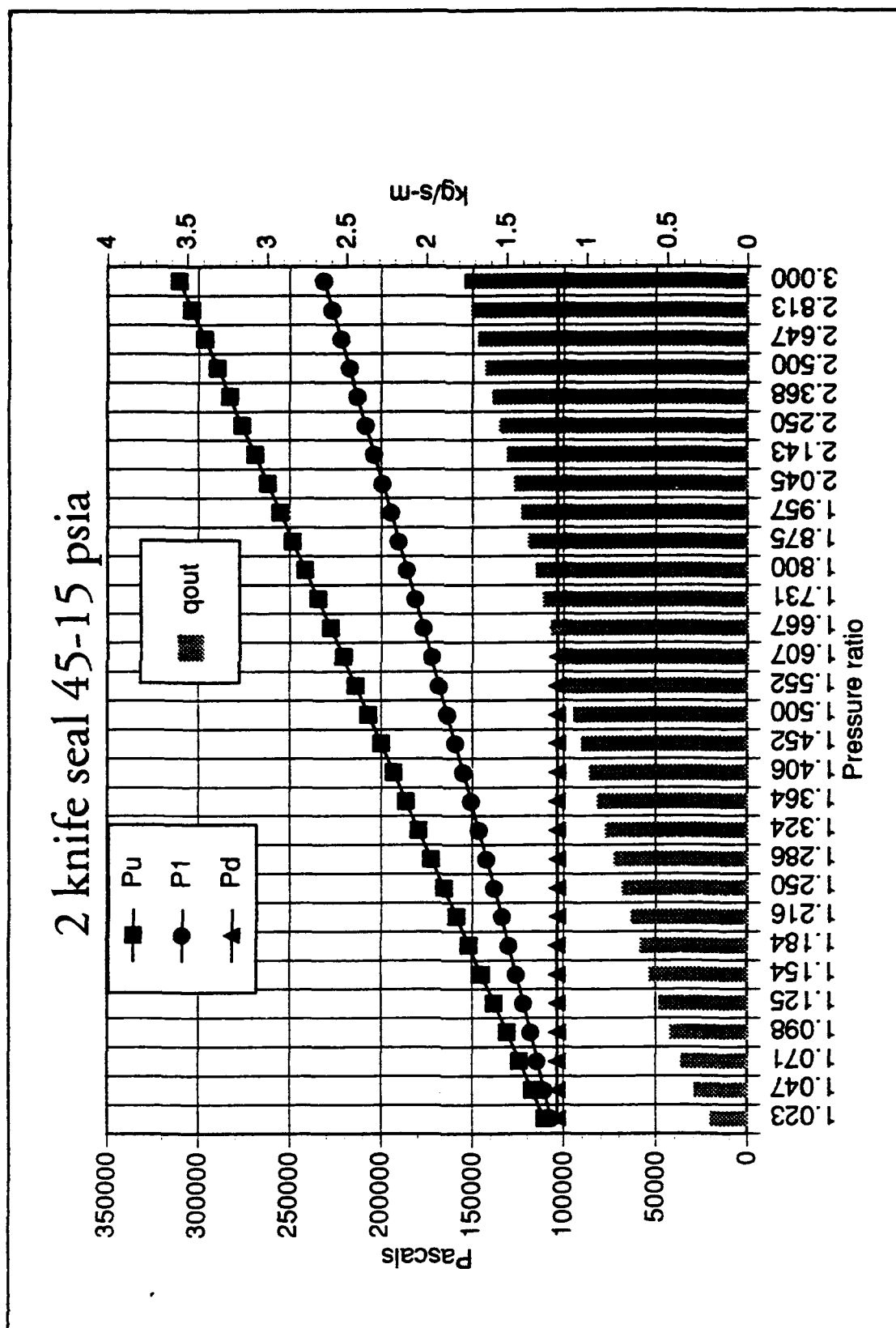


Figure 5.11 Test Rig Performance

3 knife seal 45-15 psia

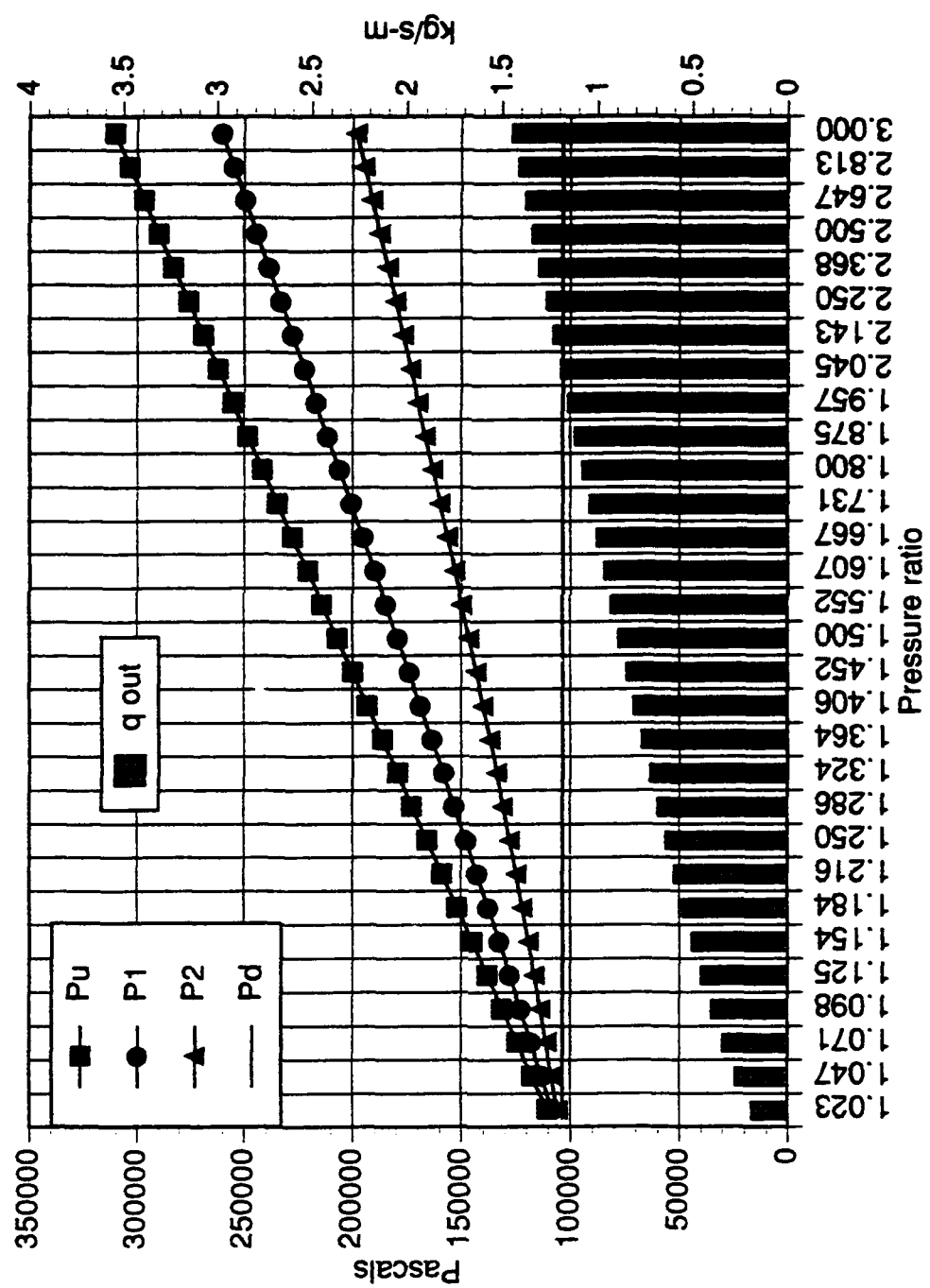


Figure 5.12 Test Rig Performance

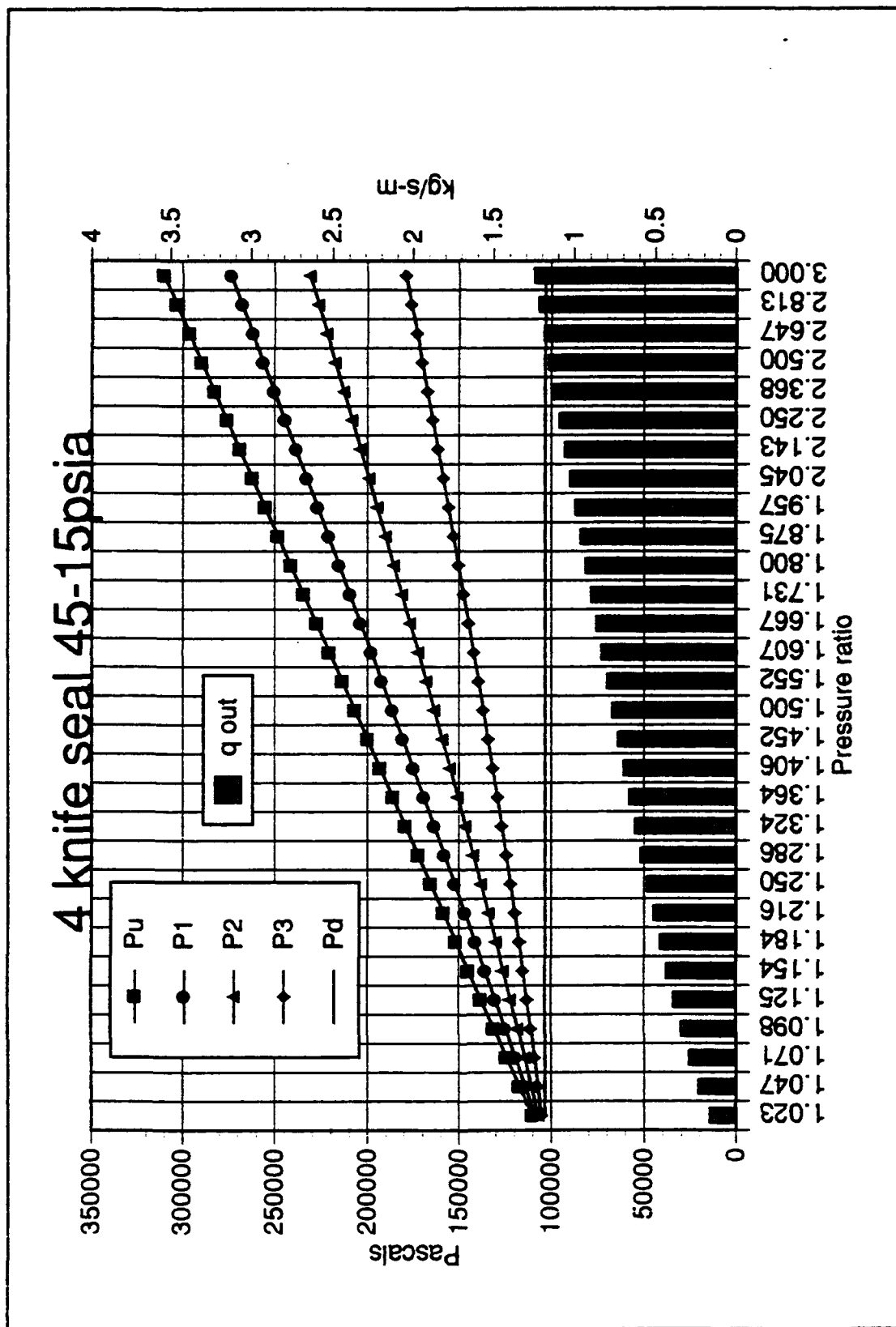


Figure 5.13 Test Rig Performance

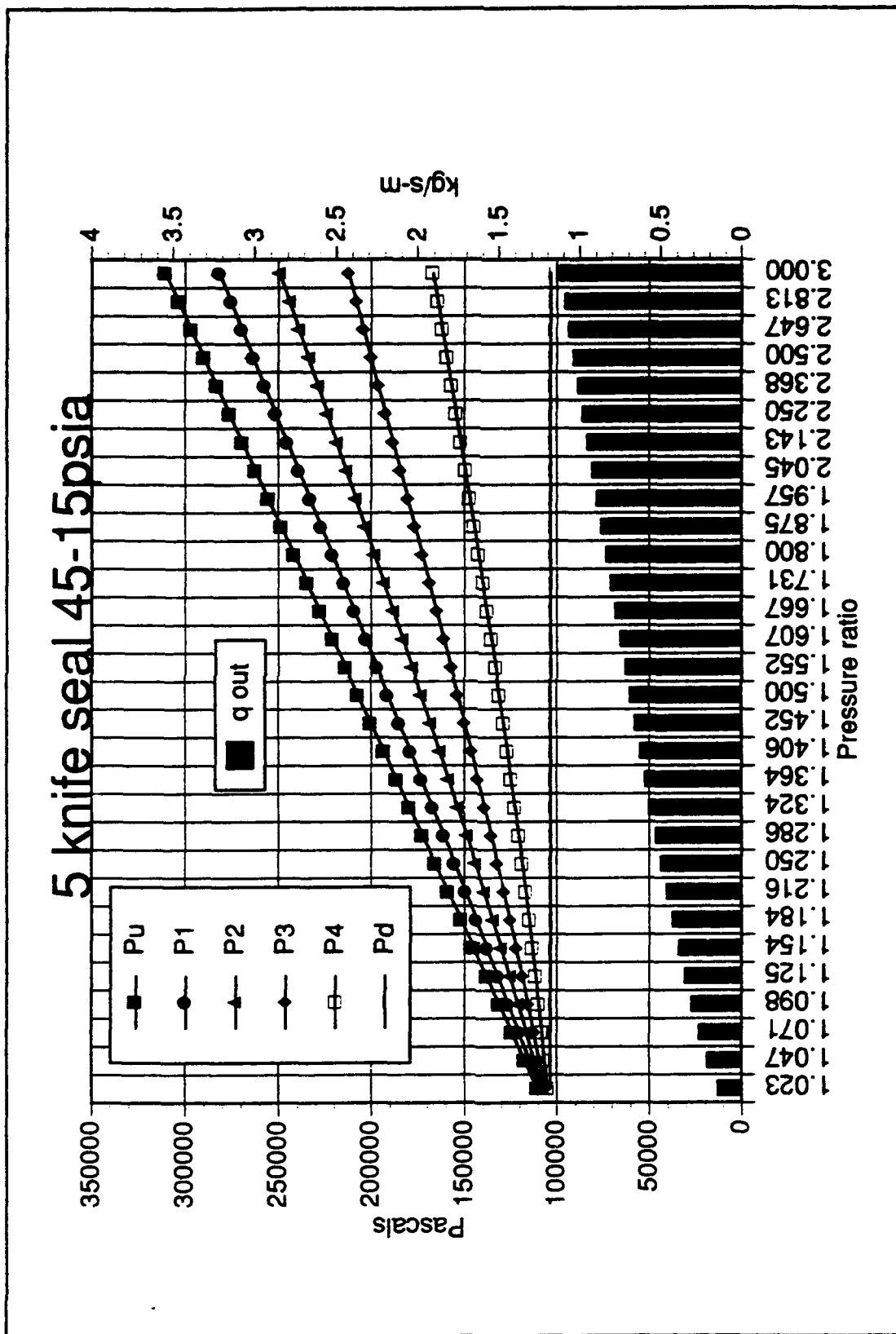


Figure 5.14 Test Rig Performance

APPENDIX A: SEAL LEAKAGE PREDICTION PROGRAM

```

%%%%%%%%%%%%%%%%%%%%%%%%%%%%%%%%%%%%%%%%%%%%%%%%%%%%%%%%%%%%%%%%%%%%%%%%%%%%%%
% This program will determine the 1-D intermediate pressures and mass flow through %
% a labyrinth seal with 2 knives. The user specifies seal gap, inlet and exit pressures, seal %
% length and pressure step size. %
%%%%%%%%%%%%%%%%%%%%%%%%%%%%%%%%%%%%%%%%%%%%%%%%%%%%%%%%%%%%%%%%%%%%%%%%%%%%%%
clear

```

```

% Specify seal gap in inches.
g=.15;

```

```

% Specify seal length in inches (Used only for BETA calculation).
L=2;

```

```

% Specify inlet pressure in psia.
po=75;

```

```

% Specify outlet pressure in psia.
pn=15;

```

```

% Specify pressure step size in psia
stepsize=2

```

```

N=(po-pn)/stepsize

```

```

% This converts gap and length to meters.
gm=g*.0254;
Lm=L*.0254;

```

```

% This converts inlet and outlet pressures to Pascals.
pom=po*6894.76;
pnm=pn*6894.76;
stm=(pom-pnm)/N;

```

```

% This specifies gamma, R and T (in Kelvin)
R=287;
T=293;
mu1=.65;

```

```

alpha=8.52/(7.23+(Lm/gm));
beta=1/((1-alpha)^.5);
mu=.65*beta;

```

```

    for i=1:N,
        pom(i,1)=pnm+(i*stm);
        p1(i,1)=sqrt(.5*pnm^2 +.5*((pom(i,1))^2));
        q1(i,1)=((mu1*gm)/sqrt(R*T))*sqrt((pom(i,1))^2-(p1(i,1))^2);
        q2(i,1)=((mu1*gm)/sqrt(R*T))*sqrt((p1(i,1))^2-pnm^2);
    end

```

```

pom
p1
pnm
q1,q2

```

```

%%%%%%%%%%%%%%%%%%%%%%%%%%%%%%%%%%%%%%%%%%%%%%%%%%%%%%%%%%%%%%%%%%%%%%%%%%%%%%
% The following statements modify the previous program for seal knives of 3,4,and 5.
%%%%%%%%%%%%%%%%%%%%%%%%%%%%%%%%%%%%%%%%%%%%%%%%%%%%%%%%%%%%%%%%%%%%%%%%%%%%%%

```

```

% This is for 3 knives.

```

```

for i=1:N,
    pom(i,1)=pnm+(i*stm);
    p1(i,1)=sqrt((1/3)*pnm^2 + (2/3)*(pom(i,1))^2);
    p2(i,1)=sqrt((2/3)*pnm^2 + (1/3)*(pom(i,1))^2);

    q1(i,1)=((mu1*gm)/sqrt(R*T))*sqrt((pom(i,1))^2-(p1(i,1))^2);
    q2(i,1)=((mu1*gm)/sqrt(R*T))*sqrt((p1(i,1))^2-(p2(i,1))^2);
    q3(i,1)=((mu1*gm)/sqrt(R*T))*sqrt((p2(i,1))^2-pnm^2);
end

```

```

% This is for 4 knives.

```

```

for i=1:N,
    pom(i,1)=pnm+(i*stm);
    p1(i,1)=sqrt(.25*pnm^2 + .75*(pom(i,1))^2);
    p2(i,1)=sqrt(.5*pnm^2 + .5*(pom(i,1))^2);
    p3(i,1)=sqrt(.75*pnm^2 + .25*(pom(i,1))^2);

    q1(i,1)=((mu1*gm)/sqrt(R*T))*sqrt((pom(i,1))^2-(p1(i,1))^2);
    q2(i,1)=((mu1*gm)/sqrt(R*T))*sqrt((p1(i,1))^2-(p2(i,1))^2);
    q3(i,1)=((mu1*gm)/sqrt(R*T))*sqrt((p2(i,1))^2-(p3(i,1))^2);
    q4(i,1)=((mu1*gm)/sqrt(R*T))*sqrt((p3(i,1))^2-pnm^2);
end

```

```

% This is for 5 knives.

```

```

for i=1:N,
    pom(i,1)=pnm+(i*stm);

    p1(i,1)=sqrt(.2*pnm^2 + .8*(pom(i,1))^2);
    p2(i,1)=sqrt(.4*pnm^2 + .6*(pom(i,1))^2);
    p3(i,1)=sqrt(.6*pnm^2 + .4*(pom(i,1))^2);
    p4(i,1)=sqrt(.8*pnm^2 + .2*(pom(i,1))^2);

    q1(i,1)=((mu1*gm)/sqrt(R*T))*sqrt((pom(i,1))^2-(p1(i,1))^2);
    q2(i,1)=((mu1*gm)/sqrt(R*T))*sqrt((p1(i,1))^2-(p2(i,1))^2);
    q3(i,1)=((mu1*gm)/sqrt(R*T))*sqrt((p2(i,1))^2-(p3(i,1))^2);
    q4(i,1)=((mu1*gm)/sqrt(R*T))*sqrt((p3(i,1))^2-(p4(i,1))^2);
    q5(i,1)=((mu1*gm)/sqrt(R*T))*sqrt((p4(i,1))^2-pnm^2);
end

```

APPENDIX B: LIST OF MATERIALS

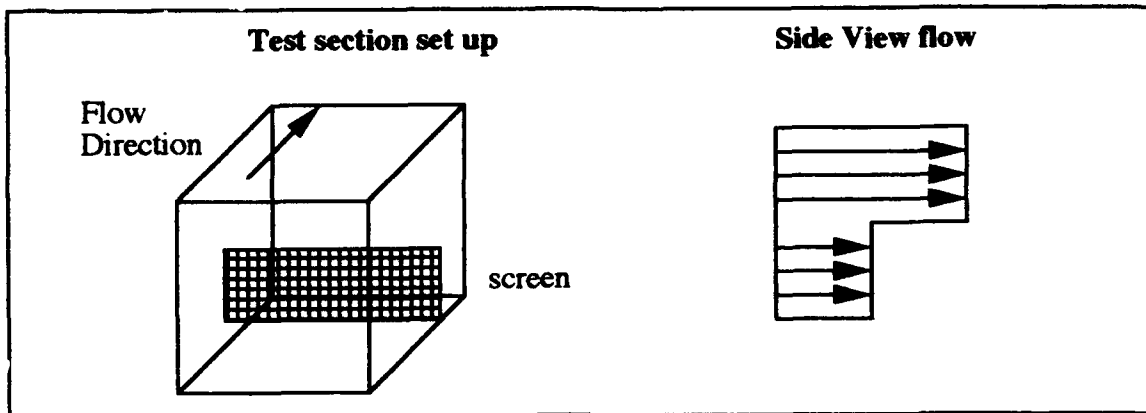
Air flow piping and valves		
Quantity	Description	Approximate cost
		(Dollars)
20 FEET	PVC SCHED 80, 2" ID	\$40
10 FEET	2" STEEL PIPE	\$100
1	FLANGE CONNECTION	\$50
1	MANUAL SHUT OFF VALVE 2" GLOBE FULL PORT	\$75
1	ADJUSTABLE PRESS REG VALVE 0-45 PSIG, FULL PORT, TIGHT SHUT OFF	\$2,300
1	PRESSURE RELIEF VALVE, ADJUSTABLE 35-50 PSIG	\$150
1	EXIT VALVE, 4" BUTTERFLY OR GLOBE, FULL PORT	\$250
1	FILTER ASSEMBLY GP198-0030-020	\$900
Diffuser assembly		
Quantity	Description	Approximate cost
		(Dollars)
1	1" STEEL PLATE 9.25"X18.5"	\$30
1	1" STEEL PLATE 0.75"X18.5"	\$30
1	1" STEEL PLATE 33.75"X20"	\$30
1	1" STEEL PLATE 34.75"X22"	\$30
2	1" STEEL PLATE 0.75"X22"	\$30
2	1" STEEL PLATE 0.75"X10.25"	\$30
20	0.375" X3" BOLTS	\$5
36	0.5"X3" BOLTS	\$5
1	0.25" 36"X18" STEEL PLATE	\$30
2	SCREEN/HONEYCOMB ASSEMBLIES	\$30

Contraction assembly		
Quantity	Description	Approximate cost
		(Dollars)
2	0.5" STEEL PLATE 9"X17"	\$20
2	0.5" STEEL PLATE 18"X18"	\$20
1	0.75" STEEL PLATE 1.5"X22"	\$10
1	0.75" STEEL PLATE 2.5"X22"	\$10
2	1" STEEL PLATE 0.75"X10"	\$10
18	0.375" X3" BOLTS	\$5
Settling assembly		
Quantity	Description	Approximate cost
		(Dollars)
2	0.5" STEEL PLATE 2.5"X5"	\$10
2	0.5" STEEL PLATE 5"X18"	\$20
2	0.5" STEEL PLATE 5"X19"	\$20
2	0.5" STEEL PLATE 4.5"X1"	\$10
18	0.375" X3" BOLTS	\$5
Test Section		
Quantity	Description	Approximate cost
		(Dollars)
2	1.5" STEEL PLATE 2.5"X8"	\$30
1	0.5" STEEL PLATE 8"X18"	\$25
2	0.5" STEEL PLATE 7"X1.5"	\$20
2	0.5" STEEL PLATE 1"X18"	\$25
64	0.375" X3" BOLTS	\$20
3	1"X4"X6" glass plate	\$150

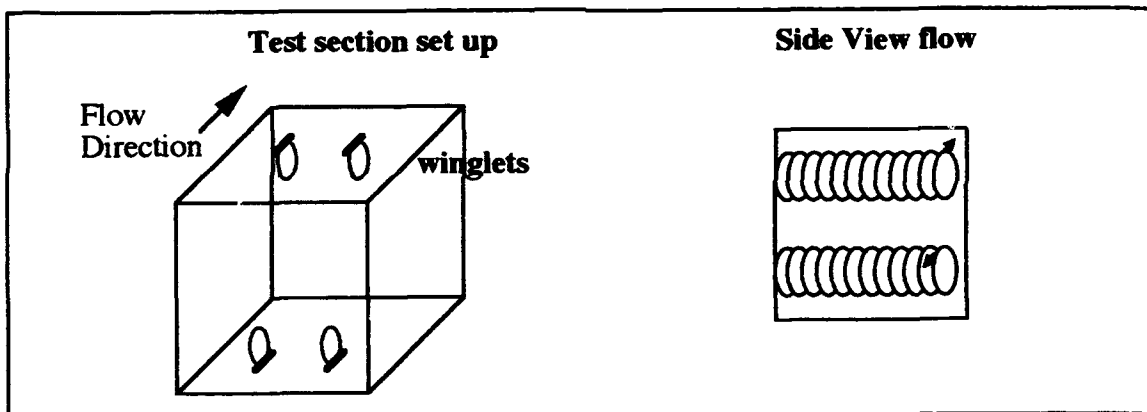
Exit Section		
Quantity	Description	Approximate cost
		(Dollars)
2	0.5" STEEL PLATE 10"X19"	\$30
2	0.5" STEEL PLATE 4"X10"	\$25
2	0.5" STEEL PLATE 1"X4.5"	\$20
2	0.5" STEEL PLATE 1"X19"	\$25
1	4" steel pipe, 5" in length	\$5

APPENDIX C: FLOW MODIFICATIONS

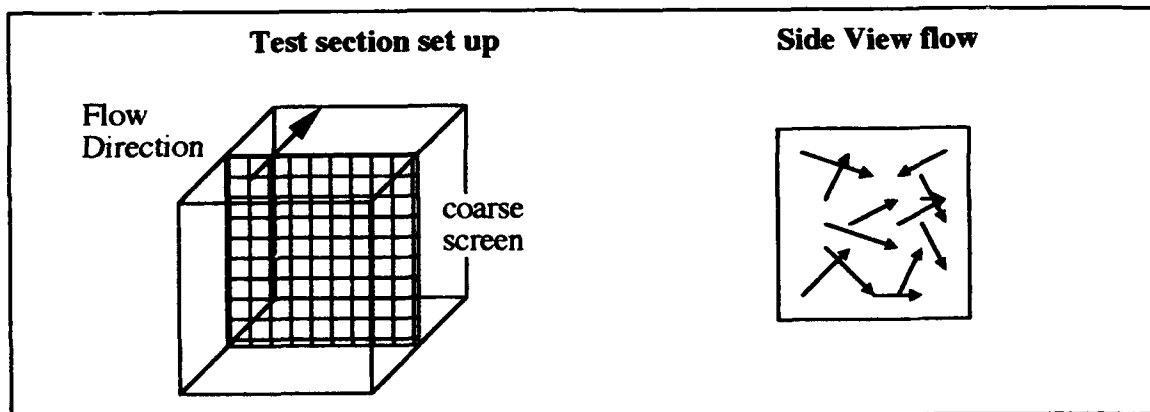
SHEAR



VORTEX



TURBULENT



REFERENCES

1. Wrigley, B., Technical Evaluation Memorandum Advisory Group for Aerospace Research and Development (AGARD), 1978, Report No CP-237.
2. Sneck, H.J., Labyrinth Seal Literature Survey Journal of Lubrication Technology Oct 1974, pp. 579-581.
3. Parsons, C.A., The Labyrinth Packing Engineer Vol 165, No 4280 Jan 1938, pp. 23-84.
4. Martin, H.M., Labyrinth Packings Engineering, Jan 1908, pp. 35-36.
5. Gercke, M.J., Berechnung der Ausflussmengen von Labyrinth Dichtungen. Die Wärme Vol 57, 1934, pp. 413-417. Also Mechanical Engineering, Vol 56 1934, pp. 678-680.
6. Egli, A. The Leakage of Steam Through Labyrinth Seals Trans. ASME Vol 57 1 1935, pp. 115-122.
7. Hodkinson, B., Estimation of the Leakage Through a Labyrinth Gland Proc. Inst. Mech. Engrs. Vol 141, 1939, pp. 283-288.
8. Jerie, J., Flow Through Straight-Through Labyrinth Seals Proc. of 7th Int'l Congress for Applied Mechanics, Vol 2, 1948, pp. 70-82.
9. Kearton, W.J. and Keh, T.H., Leakage of Air Through Glands of Staggered Type Proc. Inst. of Mech. Engrs., Vol 166, 1952, pp. 180-195.
10. Zabriskie, W. and Sternlicht, B., Labyrinth Seal Leakage Analysis Journal of basic engineering, Vol 81, 1959, pp. 332-340.
11. Vermes, G., A Fluid Mechanics Approach to the Labyrinth Seal Leakage Problem Journal of Engineering for Power, Apr 1961, pp. 161-169.
12. Stocker, H.L., Aerodynamic Performance of Conventional and Advanced Design Labyrinth Seals with Solid-Smooth, Abradable, and Honeycomb Lands NASA report CR 135307, Nov 1978, pp. 1-143.
13. Pope, M.S., Wind Tunnel Testing John Wiley & Sons, 1954, pp. 60-111.
14. Hornung, H., CALTECH, Diffuser Design and Flow Modification Personal Phone Conversation of 28 Oct 1993, (818)395-4551.
15. White, Fluid Mechanics McGraw-Hill 1986, pp. 113-511.
16. Roark, R.J., Formulas for Stress and Strain McGraw-Hill 1982, pp. 324-414.
17. Shigley, J.E. and Mischke, C.R., Mechanical Engineering Design McGraw-Hill 1989, pp. 3-25, pp. 325-383.

18. Dryden, H.L. and Abbott, I.H., The Design of Low Turbulence Wind Tunnels TR 940, 1949.
19. Lamb, H., Hydrodynamics, 6th edition, Dover, 1932, pp. 96-98.

INITIAL DISTRIBUTION LIST

	No. Copies
1. Defense Technical Information Center Cameron Station Alexandria, Virginia 22314-6145	2
2. Library, Code 0142 Naval Postgraduate School Monterey, California 93943-5100	2
3. Department Chairman, Code ME Department of Mechanical Engineering Naval Postgraduate School Monterey, California 93943-5000	1
4. Professor Knox T. Millsaps, Code ME/MI Department of Mechanical Engineering Naval Postgraduate School Monterey, California 93943-5000	5
5. LT Joseph S. Konicki 8218 Oak Moss Spring, Texas 77379	4
6. Curricular Officer, Code 34 Department of Mechanical Engineering Naval Postgraduate School Monterey, California 93943-5100	1